Simulations and experimental study to compare the behavior of a genset running on gasoline and syngas for small scale power generation

Carlos Vargas-Salgado[a], Jesús Águila-León[a,b], David Alfonso-Solar[a], Anders Malmquist[c].

[a] Instituto de Ingeniería Energética, Universitat Politècnica de València, Valencia, Spain.
[b] Departamento de Estudios del Agua y la Energía, Universidad de Guadalajara, México.
[c] Department of Energy Technology, KTH Royal Institute of Technology, 100 44 Stockholm, Sweden.

1. Abstract

Syngas produced from small-scale biomass gasification plants (tens of kW) can generate power from biomass resources. However, due to the syngas gensets demand is marginal, compared to gasoline gensets, it is not easy to find a genset specially designed to run on syngas. In this paper, an experimental study of a genset running on two kinds of fuel has been carried out. The genset used is a 10 kW ICE initially designed to run on gasoline, in parallel, simulations based on CHEMKIN-PRO software were made. The study focuses on the comparison of the ICE operation independently working on gasoline and syngas. Modifications were required in the genset to adapt the intake system to run on syngas. The syngas is obtained from a gasifier. According to the test, it is possible to convert a gasoline engine to a 100% syngas engine through straightforward modifications in the inlet manifold but reducing the efficiency and power. The electrical power running the genset on gasoline was 6.7 kW, whereas, with syngas, it is 4.8 kW (31.4% of reduction). The efficiency running the ICE on gasoline was 13.7% at its rated power, whereas for the genset fuelled on syngas, it was 10.5% (23.4% reduction).

Keywords: Syngas, Gasoline, Genset, Power Generation.

---

[a] corresponding author

Email addresses: carvarsa@upvnet.upv.es (C. Vargas-Salgado), jesus.aguila@academicos.udg.mx (J. Águila-Leons), daalso@iie.upv.es (D. Alfonso-Solar), andmal@kth.se (A. Malmquist)

Nomenclature	
CR	Compression ratio
EA	Excess air %
ER	Equivalence ratio, actual air/fuel ratio to the stoichiometric air/fuel ratio
P_{i_g}	Gasoline input power in kW
$P_{i_{sg}}$	Syngas input power in kW
ER	Equivalence ratio
LHV_{m_g}	Lower heating value of gasoline-air mixture in MJ/Nm^3
LHV_{m_sg}	Lower heating value of syngas-air mixture in MJ/Nm^3
LHV_{sg}	Lower heating value of the Syngas MJ/Nm^3
LHV_g	Lower heating value of gasoline in MJ/kg
$\dot{m}_g$	Instantaneous mass flow of gasoline in kg/h
$\dot{Q}_a$	Airflow in Nm^3/h
$\dot{Q}_m$	Mixture air/fuel flow Nm^3/h
$\dot{Q}_{sg}$	Syngas flow Nm^3/h
V_{sto_a}	Volume of the stoichiometric air in Nm^3
$(A/F)_{st}$	Stoichiometric Air /Fuel relation
ρ_a	Air density in kg/m^3
η_g	Gasoline mode overall efficiency in %
η_{sg}	Syngas mode overall efficiency in %
AFV	Adiabatic flame temperature
CDI	Capacitor discharge ignition
BTDC	Before the top dead center
ICE	Internal Combustion Engine
LHV	Lower heating value
OHV	Overhead valve
RES	Renewable energy sources
SI-ICE	Spark-ignition internal combustion engine
TDC	Top dead center

2. Introduction

Nowadays, climate change and its effects are a reality, and the continued consumption of electricity demand and its associated pollution is a significant problem [1]. It has been estimated that almost 76% of the total energy consumed globally comes from fossil fuels [2]. One way to mitigate climate change is through technologies and practices that reduce CO_2 emissions [3]. An alternative to fossil fuels is renewable energy sources (RES); however, most RES has the disadvantage of having a significant variability in terms of energy production. For example, solar photovoltaic and plastic technologies rely heavily on environmental conditions [4]. A storage system like batteries is an expensive solution. For continuous power generation purposes from renewable energy sources without depending on the weather conditions, biomass gasification is a technology to consider [5]. Since the biomass can be stored, a biomass gasification plant could be integrated into a stand-alone hybrid microgrid to increase the system's feasibility [6–10]. In 2016 about 2%, this is 500 TWh, from the energy generated worldwide came from biomass [11], and it is estimated that by 2060 biomass will provide about 17% of the global total energy demand [12].

In recent years, gasified biomass for energy production has a renewed interest due to its lower environmental impact than other sources such as biomass incineration for power generation [13]. Syngas (synthesis gas) is a fuel obtained from biomass gasification, and it has research interest nowadays [14]. Syngas is a mixture of different gases, and his typical molar composition is 15-20% H_2, 15-30% CO, 1-5% CH_4, 7-12% CO_2, and N_2 balanced, with a heating value (HHV) ranged from 5 to 6.5 MJ/Nm^3 [15–17]. The presence of H_2 in the composition of the syngas accelerates the laminar flame speed and improves its flammability compared to biogas, which reduces engine emissions [18]. Removal of impurities, such as tars, from the obtained syngas is necessary to burn it in an ICE typically operated with gasoline.

Following some modifications, the ICE would be able to run on syngas as a primary fuel for power generation purposes [19,20].

Multiple studies have analyzed the use of syngas in internal combustion engines for power generation purposes [15,21–26]. Other studies focus on the use of a syngas-diesel mix, taking advantage of a diesel generator high compression ratio to increase the thermal efficiency, obtaining a reduction in NO_x and CO_2 emissions compared to natural gas [3,17,27,28]. Other authors use different combinations of syngas with methane, biogas, and hydrogen [26,29,30]. Monteiro et al. analyses the use of syngas in a rapid compression machine [31]. Shivapuji and Dasappa study the concentration of H_2 in the syngas used to run an ICE [26]. Also, some authors use models to simulate the pure syngas combustion behavior compared to methane or mixed with diesel [32,33]. Finally, Fiore et al. work on a detailed review of the ICE powered by syngas [34]. A summary of the previous scientific works is shown in Table 11 in Annex I.

In this work, syngas was obtained from a downdraft gasifier using woodchips as a primary fuel. A sensitivity analysis of the results is developed in section 5. Such analysis compares and gives information about the laminar flame velocity, adiabatic flame temperature, and the emissions as a function of the ER in both fuels. Also, efficiency, power, and torque as a function of ER and ignition timing are analyzed. Finally, it was studied the evolution of the cylinder pressure to crank angle. All this information plays an important role in the design of a syngas ICE. Engine efficiency study is developed through tests. The data for the analysis were obtained from the measuring device located in the experimental plant, composed of a downdraft gasifier and a modified ICE able to run independently on syngas or gasoline. Compared to gasoline gensets, the demand market for syngas gensets is marginal. It is not easy to find a small-scale genset specifically designed to run on syngas. This work arises from the impossibility of finding on the market an engine capable of operating on the syngas produced in a small-scale biomass

gasification plant. Hence, the work aims to verify the technical viability of running on syngas without substantial modifications; an ICE initially intended to run on gasoline. The novelty of the results is focused on this point. A sensitivity analysis is required to investigate the operation conditions, the behavior, and the ICE response to reach the goal. Because the final solution's cost is a decisive factor in making a biomass gasification power plant profitable, the conversion must be developed quickly and easily, without significant and expensive modifications. The only developed amendment was the admission system's adaptation. Because it requires a substantial change in the engine design, the compression ratio was no altered.

Due to the complex operation of an ICE, the test has been complemented through simulations. Because it is widely used in the scientific field for combustion process analysis [33,35–40], CHEMKIN-PRO [41] was employed to simulate the combustion process of the ICE analyzed. CHEMKIN-PRO is used by [42] to analyze the behavior of a dual-fuel engine using gasoline and diesel, also [43] develops simulations of a biodiesel engine using a parallel surrogate optimization algorithm. Besides, several works analyze the use of syngas in an ICE to estimate the laminar burning velocity [44] and to test a dual fuel engine [32,45]. In this work, CHEMKIN-PRO is used to carry out a sensitive analysis and compare experimental tests and simulations.

3. Experimental setup

3.1. Biomass gasification plant

A downdraft gasifier was used to produce syngas to run an ICE for power generation purposes. Downstream of the reactor, gas cleaning, and the cooling system were installed to clean the gas, reaching the required quality (

Fig. 1).

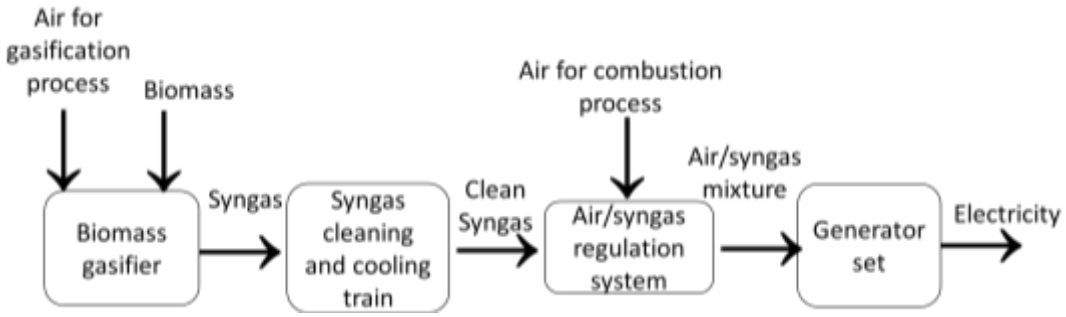

Fig. 1. General scheme of the experimental setup.

The four steps of the gasification process are carried out into the reactor (drying, pyrolysis, combustion, and reduction, see Fig. 4), producing syngas to run an ICE after a cleaning process. The downdraft gasification reactor has an essential advantage in power generation applications: the syngas tar concentration is smaller than other technologies. A significant part of tars produced in the pyrolysis process is cracked when the syngas goes across the throat (which is the part of the reactor with the smallest area). Despite such advantages, a cleaning system is required to remove ash, remaining tar, and unreacted carbonaceous material. The main components of the gasifier are shown in Fig. 2, Fig. 3, and Table 1.

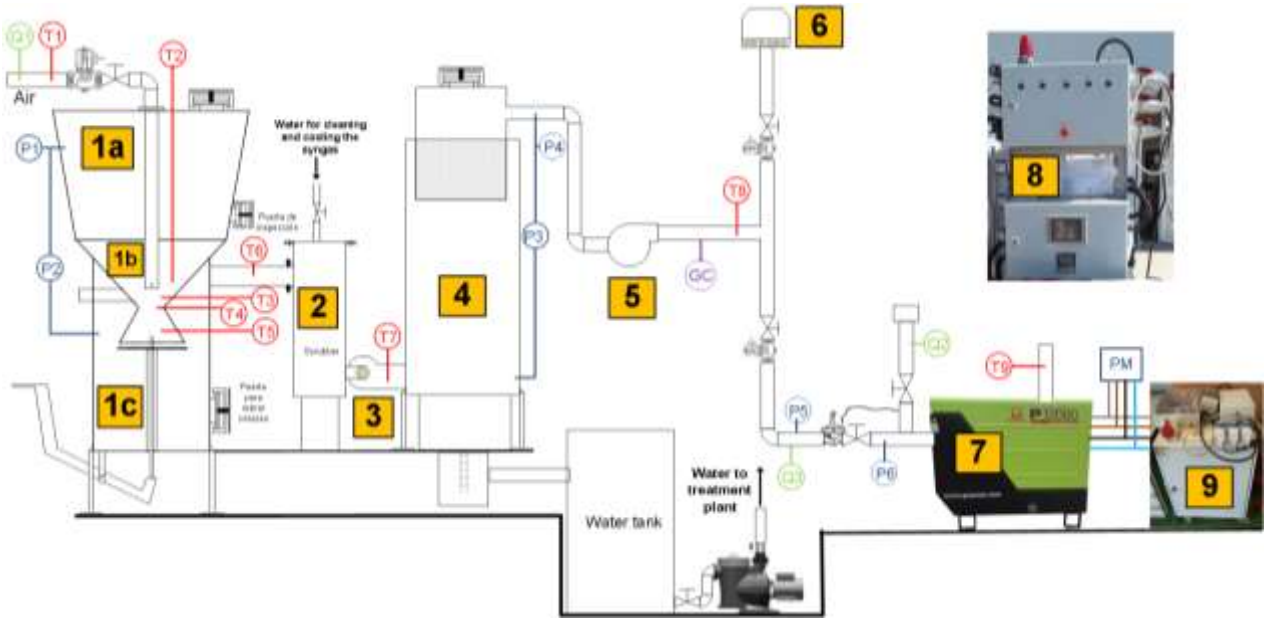

Fig. 2. Diagram of the experimental setup and components.

Table 1. Main components of the biomass gasification plant.

	Components of the plant
1a	Reactor (Biomass zone)
1b	Reactor (Reactions zone)
1c	Reactor (Ash zone)
2	Scrubber
3	Centrifugal tar separator
4	Filter
5	Vacuum pump
6	Torch
7	Internal combustion engine
8	Electrical box – control panel
9	Electric programable load

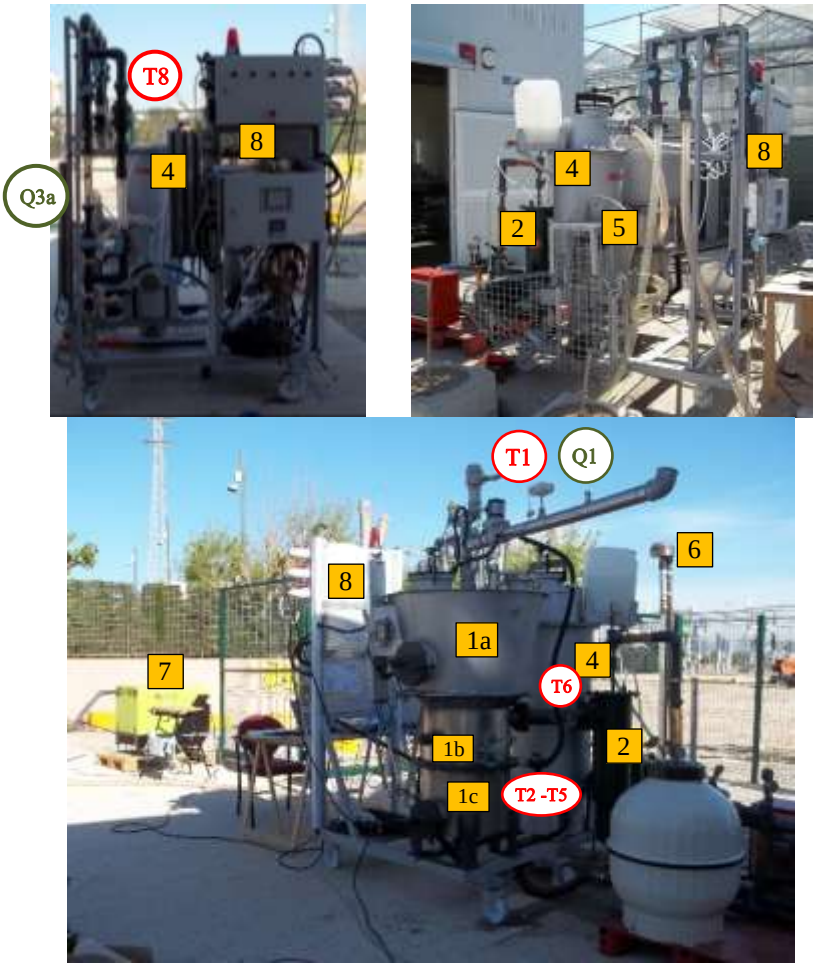

Fig. 3. Pictures and components of the biomass gasification plant. Front view (Left up) and rear sight (Right up and down).

The datasheet of the biomass gasification plant is shown in Table 2. The genset efficiency depends significantly on the kind, size, air or water-cooled, efficiency of the alternator, and design quality of the genset. According to market availability, the small-scale gasoline genset

efficiency goes from 13 to 23%, and this value could be reduced to around 30% if the engine is adapted to run on syngas.

Table 2. Datasheet of the biomass gasification plant used for the simulations [9]**.**

Biomass gasifier (reactor type)	**Fixed-bed downdraft**
Reactor material	Stainless Steel
Fuel type	Wood chips, wooden block < 5–40 mm
Gasification Agent	Air
Airflow required by the gasification process	8 – 15 m^3/h
Biomass hopper capacity	226 liter (45 kg, bulk density: 200 kg/m^3)
Biomass consumption	5 to 10 kg/h
Syngas production	12 – 28 Nm^3/h
Syngas Lower Heating Value	5–5.8 MJ/Nm^3
Thermal power	17 - 42 kW_{th}
Efficiency (biomass to syngas)	60-79%
Bed pressure drop (throat zone)	0.4 – 1.2 kPa

The tar formation process and the profile temperature into the reactor are shown in Fig. 4. The highest temperature occurs in the reactor's combustion zone, where the throat (reactor's smallest section) is located. In this zone, the tars cracks, provoking its concentration in the syngas to decrease.

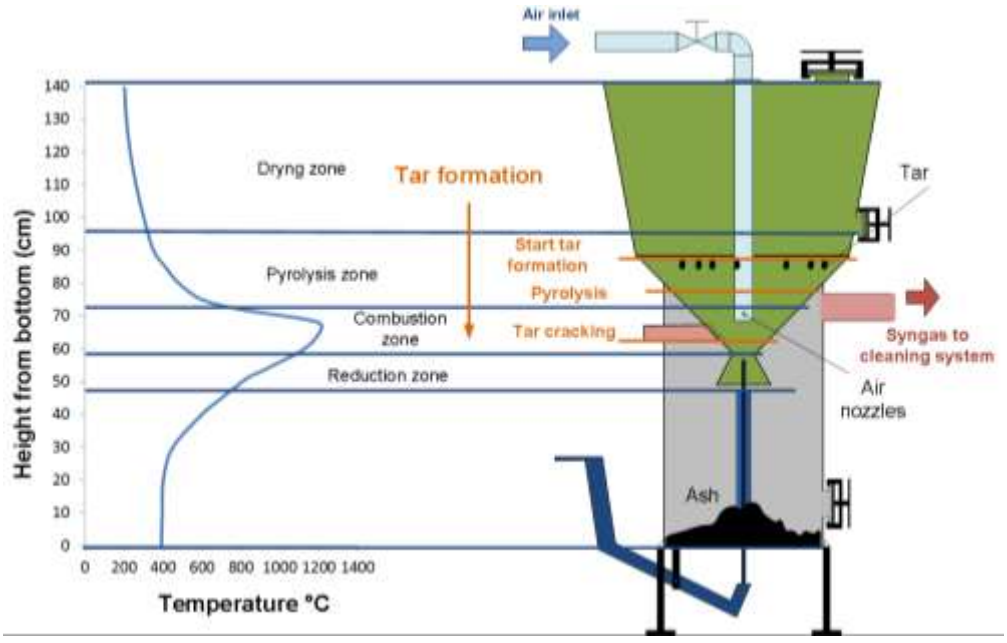

Fig. 4. Tar formation and temperature profile into the reactor (adapted from [46]**)**

3.2.Properties of the biomass used and produced syngas.

Properties of the biomass used are shown in Table 3. Characteristics of the syngas produced are shown in Table 4. The produced syngas is free of tars and suspended particulates. There was not available a device to measure the tar, humidity, and suspended particulates concentration. The way to determine if the quality of gas was adequated was by a visual inspection, initially every ten operating hours in two specific points: the syngas filter at the engine inlet and the transparent methacrylate pipe (number 6 in Fig. 5 and Fig. 6).

Table 3. Characteristics of biomass.

Property		Value
Type of biomass		Woodchips
Bulk density Stored biomass (kg/m^3)		200
LHV (MJ/kg)		16.24
Ultimate analysis %	C	52%
	H	6%
	O	42%
Proximate analysis %	Fixed carbon (FC)	9%
	Volatile	83%
	Ash	1%
	Moisture	7%

Table 4. Characteristics of the syngas produced and gasoline.

Property	Value
Syngas LHV MJ/m^3	5.4
Syngas Density (kg/m^3)	0.95
Gasoline LHV MJ/kg	44.3
Syngas composition (dry)	
CO_2 %	11.3
N_2 %	48.6
CO %	22.2
CH_4 %	2.8
H_2 %	15.1

An alternative method used was the opacimeter technique, typically used to carry out a smoke test and estimate the combustion process's unburned losses. Once the gasification plant cleaning system was able to clean the syngas adequately, the inspection was carried out every

100 hours, and also the carburetor zone was inspected. As a result, after 500 hours of operation, not tars, water or particles were found, and the syngas was considered able to run the ICE.

3.3. Generator set

The genset used is a PRAMAC P 12000, composed of an ICE (Table 5) and a synchronous generator (Table 6).

Table 5. Details of the engine's specifications [47].

Engine specifications	
Model	Honda GX630
Engine type	OHV gasoline engine, air-cooled, 4-stroke, 90° V-twin design, horizontal shaft
Displacement	688 cm^3
Compression ratio	9.3: 1
Bore x Stroke	78 X 72 mm
Carburetor	Horizontal type, two-barrel butterfly valve, internal vent
Continued rated power (gasoline)	10.5 kW at 3000 rpm
Maximum net torque	48.3 Nm at 2500 rpm
Ignition timing	-20° referred to TDC at 3000 rpm
Ignition system	Digital CDI with variable ignition timing
Starting system	Electric starter
Fuel	Unleaded 86 octane or higher (gasoline)
Gasoline storage capacity	24 l
Cooling system	Forced air
Governor	Mechanical centrifugal

Table 6. Electrical generator specifications [48].

Electrical Power Generator Specifications	
Model	LINZ Electric E1 C11MB
Poles	2
Speed rotation (50 Hz)	3000 rpm
Nominal Voltage	115/230 V
Voltage accuracy	± 5% from the nominal voltage
Nominal frequency	50 Hz
Efficiency (at 3/4 load)	80.5%
Efficiency (at 4/4 load)	79.5%
Electric Power	10 kVA
Overload	110% of rated power for one hour in a cycle of 6 hours.

3.3.1. Conversion of the generator set

The genset was initially designed to run on gasoline; therefore, modifying the intake system to run it on syngas was necessary. The modification was carried out in the inlet manifold. It consists of a set to regulate the air/syngas mixture (Fig. 5 and Fig. 6). The pressure regulator valve (1) was installed to regulate the ER; the engine speed control (2) keeps the rpm in the set value independently of the load. The system allows the genset to run on either gasoline or syngas. If the engine works on gasoline, the air/fuel mixture system is the initial one originally integrated into the ICE, consisting of a traditional carburetor (3) and a conventional air admission system with a filter (6). When syngas feeds the ICE, the gasoline pipe's valvule (4) is closed. The gate valve (5) allows the regulation of the quantity of air going to the ICE. Before going into the ICE, the syngas goes through a filter (6) to avoid particles arrive in the engine (The same filter cleans the air when the engine works on gasoline); this filter was adapted for work in both modes (gasoline or syngas), and it is located on the top of the carburetor.

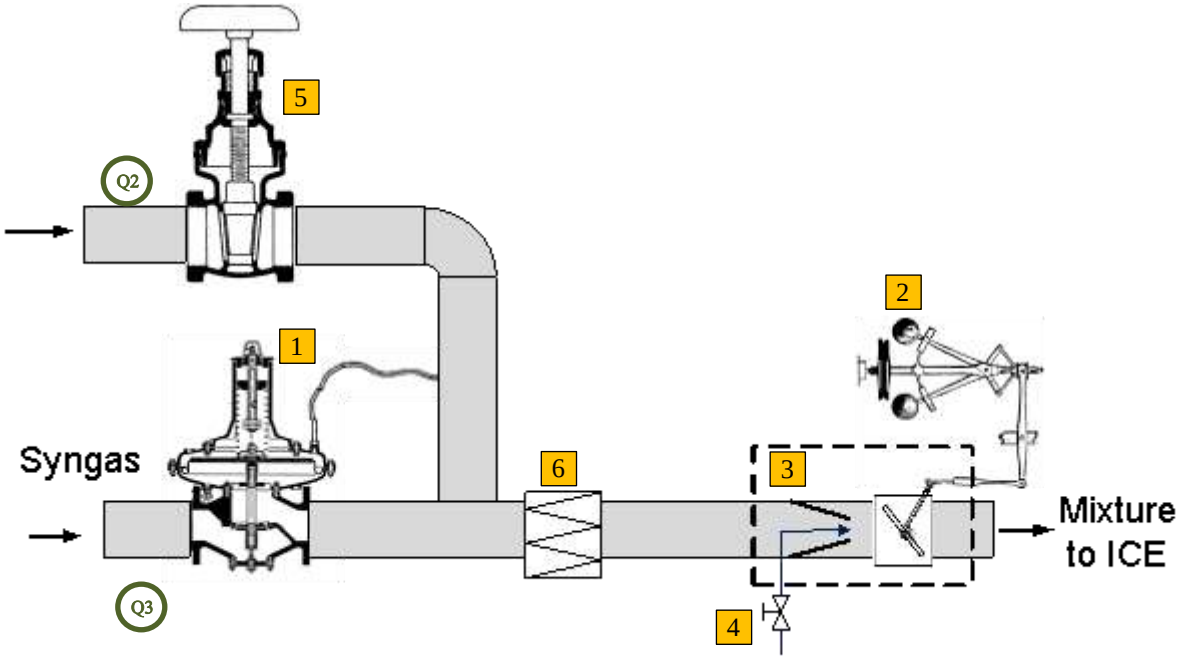

Fig. 5. Components of the syngas intake system.

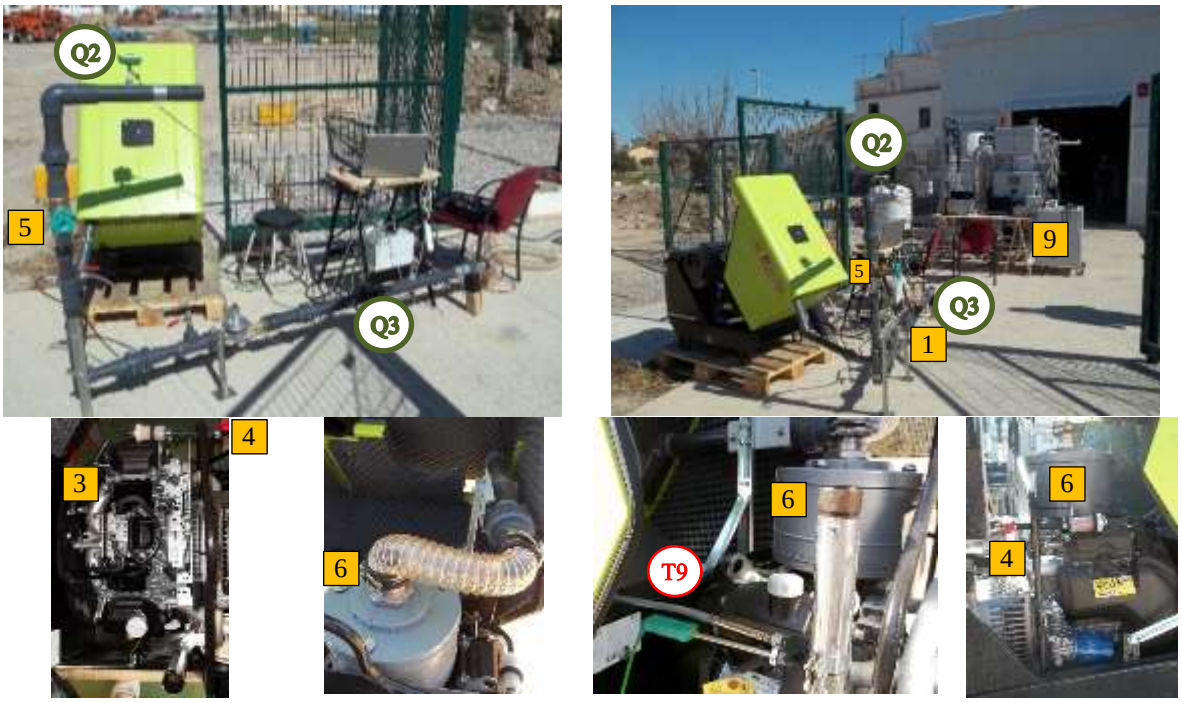

Fig. 6. Pictures of the syngas intake system adapted to gasoline genset. Components of the intake system (Up), carburetor, modified system to work on syngas, filter, thermocouple, (Down)

3.4.Measuring devices

Due to the behavior of the biomass gasification plant and reactor must be analyzed, a data acquisition system was installed. The main component of the control and data acquisition system is shown in Table 7. Table 8 shows the details of the instruments and their function, and Fig. 7 shows a scheme with the biomass gasification plant´s automation and data acquisition system.

Table 7. Equipment used during the experiment to acquire data.

Instrument	Function
2 OMRON CJ1W TS561	6 – channel input unit for K-type thermocouples
1 OMRON CJ1W AD081	8 – channel analog input unit
1 CJ1M-CPU11 OMRON SYSMAC PLC	CPU
1 OMRON CJ1W SCU31	Modbus rs 485 communication
1 OMRON CJ1M OD212	16 - transistor outputs module
1 OMRON V1000 variable speed drive	For regulating the input airflow
1 OMRON NS5 SQ10B-V2 touch screm.	HMI - Human-machine interface
SCADA CX-supervisor	HMI - Human-machine interface

Table 8. Equipment used during the experiment to acquire data.

Parameters to be measured	Abr.	Unit	Device	Signal	Accuracy
Air inlet temperature	T1	°C	Type k	mV	+/- 2.2°C or +/-0.75%
Pyrolysis zone temperature	T2	°C	Type k	mV	+/- 2.2°C or +/-0.75%
Combustion zone temperature	T3	°C	Type k	mV	+/- 2.2°C or +/-0.75%
Throat temperature	T4	°C	Type k	mV	+/- 2.2°C or +/-0.75%
Reduction zone temperature	T5	°C	Type k	mV	+/- 2.2°C or +/-0.75%
Syngas temperature at the reactor	T6	°C	Type k	mV	+/- 2.2°C or +/-0.75%
Temperature at the scrubber outlet	T7	°C	Type k	mV	+/- 2.2°C or +/-0.75%
Syngas temp. at the vacuum pump	T8	°C	Type k	mV	+/- 2.2°C or +/-0.75%
ICE exhaust temperature	T9	°C	Type k	mV	+/- 2.2°C or +/-0.75%
Biomass hopper pressure	P1	kPa	Dwyer 616K	4-20 mA	±2.0% F.S.
Bed pressure drop	P2	kPa	Dwyer 616K	4-20 mA	±2.0% F.S.
Filter pressure drop	P3	kPa	Dwyer 616K	4-20 mA	±2.0% F.S.
Pressure at the filter outlet	P4	kPa	Dwyer 616K	4-20 mA	±2.0% F.S.
Pressure at the vacuum pump outlet	P5	kPa	Dwyer 616K	4-20 mA	±2.0% F.S.
Pressure at ICE inlet	P6	kPa	Dwyer 616K	4-20 mA	±2.0% F.S.
Airflow at the reactor inlet	Q1	m^3/h	Kimo CTV 100	4-20 mA	+/-0.3m/s or +/-3%
Airflow at the ICE inlet	Q2	m^3/h	Kimo CTV 100	4-20 mA	+/-0.3m/s or +/-3%
Syngas at the ICE inlet	Q3	m^3/h	EE65 series	4-20 mA	+/-0.2m/s or +/-3%
Syngas at the filter outlet	Q3a	m^3/h	TecFLuid PT	4-20 mA	6% (qG=50%)
Syngas composition	CO, H_2, CH_4, CO_2, O_2	%	Gasboard-3100p series	rs232	CO, CO_2, CH_4 ≤ ±2%; O_2, H_2 ≤ ±3%
Electrical parameters	V, I, P, Q, S, cosφ		Siemens SENTRON	MB rs485	V, I, P,Q +/- 1%

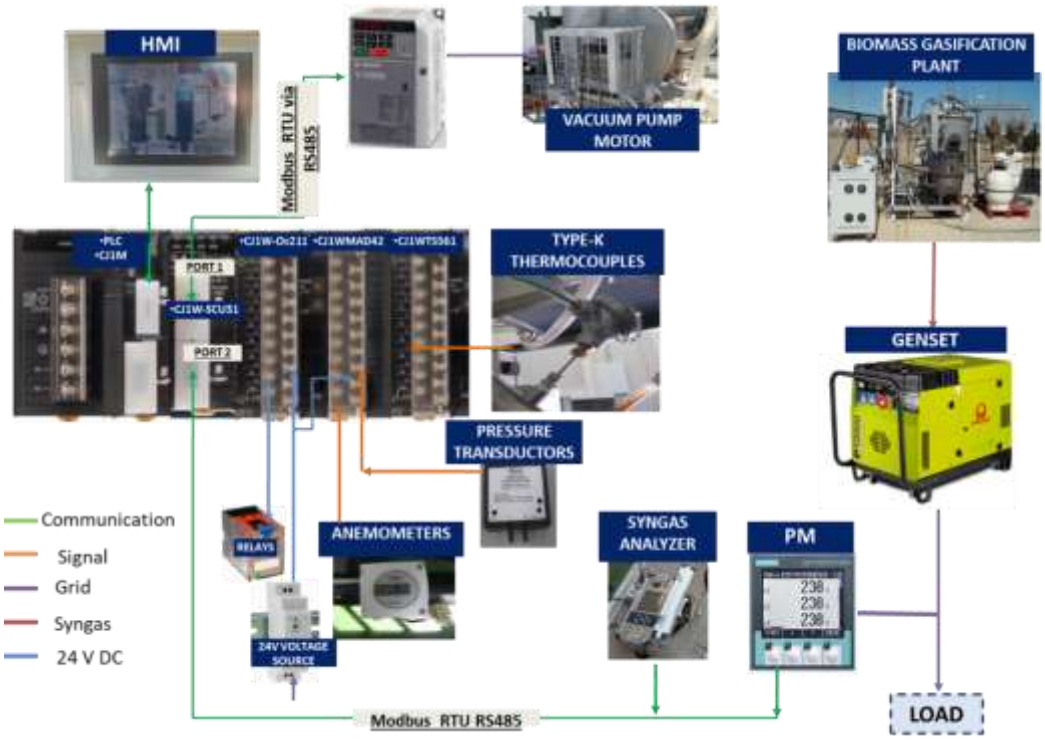

Fig. 7. Scheme of the automation and data acquisition system

4. Methodology

Many power generation options use the syngas produced in a downdraft biomass gasification plant, but the ICE is the most common. Due to its cost-benefit, it has been chosen a gasoline engine adapted to run on syngas. A methodology to compare both fuels' behavior to operate a genset is established and summarized in Fig. 8. It is mainly based on simulations through the software CHEMKIN-PRO and experimental tests. These tests required choosing the gasoline genset, adapting it to work on syngas, implementing the data acquisition system, running the engine test (on gasoline and syngas), and finally comparing and validating the results. The engine's adaptation to run on syngas and the data acquisition system was described in sections 3.3 and 3.4. Further explanation and contribution to the general methodology of simulations, tests, and calculations were detailed in sections 4.1 to 4.3.

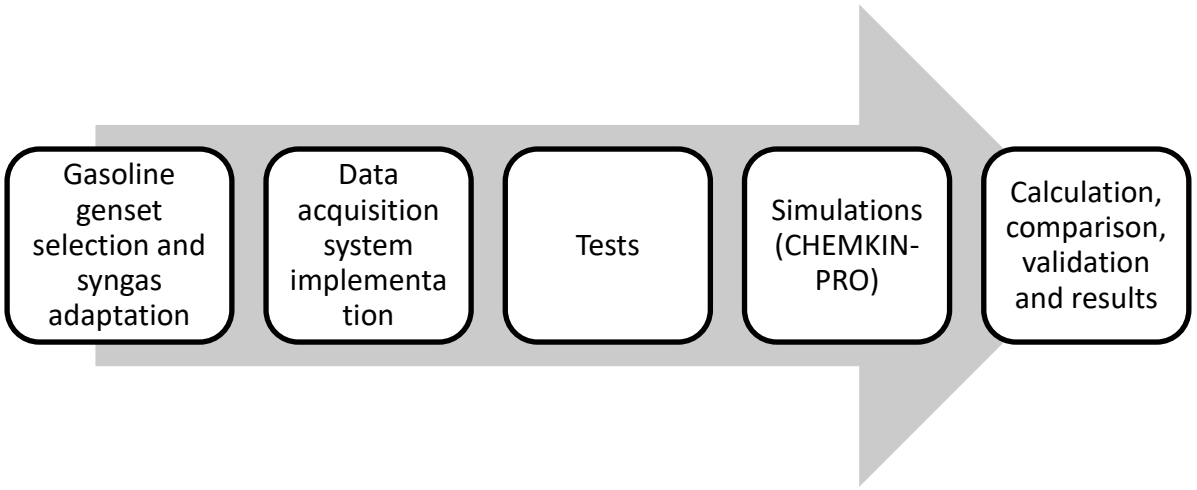

Fig. 8 Methodology carried out.

4.1. CHEMKIN-PRO simulations

Ansys CHEMKIN-PRO software package has been used for simulation purposes as it is widely used and accepted for modeling and simulating complex gas-phase chemical reactions. The performed simulations allowed us to estimate the behavior and carry out a sensitivity

analysis of the laminar flame velocity, the adiabatic flame temperature, the engine thermal efficiency, and mechanical power as a function of the equivalence ratio (ER) and the ignition timing.

4.1.1. Laminar flame velocity and adiabatic flame temperature

The adiabatic flame velocity was obtained from simulations developed in CHEMKIN-PRO. The 1-D Premixed Laminar Flame Speed Calculator module was used for that purpose. For preliminary considerations, two essential parameters for syngas and gasoline combustion processes are laminar flame velocity and adiabatic flame temperature. Main inputs for simulations are included in Table 9. Laminar flame velocity is compared for both fuels as a function of ER [49]. For gasoline, the laminar flame velocity was also obtained from previous studies reported by [50] and [51], used for comparison purposes in the results and discussion section. The chemical kinetics mechanisms used for gasoline are the NUI Galway mechanism [52], and for syngas, it was used the Gri-mech 3.0 mechanism [53].

Table 9. Laminar flame velocity input parameters

PARAMETER	VALUE
FUEL (REACTANT SPECIES)	
Gasoline composition	100% iC8H18 (ISO-OCTANE)
Syngas composition (%molar fraction)	22.2% CO ; 15.1% H_2 ; 2.8% CH_4 11.3% CO_2 ; 48.6% N_2
OXIDIZER	
Air (%molar fraction)	21% O_2 ; 79% N_2
Equivalence ratio - ER	0.9 to 1.2
INITIAL MIXTURE CONDITIONS	
Temperature	300 K
Pressure	0.1 MPa
CHEMICAL KINETICS MECHANISM	Gasoline: NUI Galway; Syngas: Gri-mech 3.0

One of the factors affecting the efficiency of the syngas engine is the adiabatic flame temperature (AFT) since higher temperature should provide higher thermal efficiency [5]

(considering the Carnot cycle as a reference). AFT is a theoretical reference and is defined as the maximum flame temperature considering complete combustion and no heat losses.

4.1.2. Power, efficiency, torque, and emissions.

The gasoline spark-ignition internal combustion engine (SI-ICE) was simulated employing the specific module included for that purpose in the CHEMKIN-PRO package, where chemical kinetics mechanisms and species thermodynamic properties are based on the previous bibliography as described in the following lines. The ICE simulation module follows a multizone model approach reported by Aceves et al. [54]. Chemical kinetics mechanisms used for the internal combustion engine's simulations were the NUI Galway mechanism developed by the National University of Ireland Galway and the Gri-mech 3.0 Mechanism developed by [55] and sponsored by the Gas Research Institute. It is explained in detail in [56]. Also, recent scientific works have used this mechanism for syngas to estimate the laminar burning velocity or simulate the combustion process [22,57–59], or for natural gas to simulate the combustion process [44,57,60]. Other mechanisms are available in the scientific bibliography, but they need to be adapted to the structure required by CHEMKIN-PRO and must also be tested [61–64]. The simulations were carried out for the real engine conditions (3000 rpm and compression ratio 9.3:1); however, to compare the engine behavior under favorable conditions for syngas, simulations were also carried out at 1500 rpm and a compression ratio of 11:1. It is well known that the knock limits the maximum CR in an ICE. Since running on syngas, the ER could reach a CR of 11:1 [34], it is not expected knocking combustion working at such CR. Main simulation inputs and boundary conditions for the operation of the SI-ICE running on gasoline and syngas are summarized in Table 10. and

The main simulation output considered for comparison purposes is the thermal efficiency of the working cycle (EFF.TH, the net work ratio from the system to the heat added to the system,

expressed in percentage) and the cycle's power (the net work from the system, expressed in kW). The model was calibrated with the engine datasheet's information (Table 5) and added thermal losses to reach the same efficiency obtained in the tests (running on gasoline and syngas). Once the model was calibrated, it analyzed the impact of CR, ignition timing, ER, and rpm on the engine performance to define the optimal operation parameters with syngas. The model's obtained power and the experimental tests were compared to verify the consistency of the results.

Table 10. SI-ICE simulation inputs.

PARAMETER	VALUE
ENGINE PHYSICAL PARAMETERS	
Engine type	4-stroque, two cylinders
Displacement	2x344 cm^3
Compression ratio	9.3: 1
Bore x Stroke	78 X 72 mm
FUEL (REACTANT SPECIES)	
Gasoline composition	100% iC8H18 (ISO-OCTANE)
Syngas composition (%molar fraction)	22% CO ; 15% H_2; 2.9% CH_4
	11% CO_2; 0.04% O_2; 48.5% N_2
OXIDIZER	
Air (%molar fraction)	21% O_2; 79% N_2
Equivalence ratio - ER	0.8 to 1.2
INITIAL MIXTURE CONDITIONS	
Temperature	373 K
Pressure	0.1 MPa
SIMULATIONS CARRIED OUT	
Start of combustion	-60 to -15° (syngas), -30 to -10° (gasoline)
Starting crank angle	-120.2°
End of simulation crank angle	-139.8
Speed engine	1500 and 3000 rpm
Compression ratio	9.3 and 11
CHEMICAL KINETICS MECHANISM	Gasoline: Galway; Syngas: Gri-mech 3.0

To have a more complete evaluation, it will be included typical SI-ICE performance indicators like NO_x, torque and cylinder pressure as a function of the crank angle. These

indicators provide both further performance information and additional validation of simulation results, as they will be compared with previous bibliography and manufacturer specifications.

Regarding torque and cylinder pressure, for torque it is directly related with mechanical power for a fixed engine specifications and shaft dimensions, and for cylinder pressure it is expected both higher power and efficiency when higher pressure is reached in the cycle [15,65,66].

Regarding NO_x emissions, it is related to temperature, so a higher temperature inside the engine should produce higher NO_x emissions [19,67] Despite it is a theoretical reference, the higher adiabatic flame temperature should also indicate higher NO_x emissions. In point 5.1.4 it is shown emissions according to simulations and comparison with the previous bibliography.

4.2.Experimental tests

The gasification plant requires about 15-20 minutes to start up. Tests were carried out once the biomass gasification plant produced syngas with adequate quality (more than 5 MJ/Nm^3) and after a reasonable time (about 10 minutes) of engine operation. The tests consisted of increasing the power demand by 1 kW every 5 minutes (starting without load) until the engine is not able to feed the load. During the test period, the data acquisition system was storing the information every 5 seconds.

4.3. Calculations

4.3.1. Power output and efficiency

It is possible to predict the electrical power output reduction when changing fuel, just considering the fuel composition [17,18,68,69]. The mixture of air/fuel flow $\dot{Q}_m$ is given by Equation (1):

$$\dot{Q}_m = \dot{Q}_{sg} + \dot{Q}_{sto\_a}(1 + EA) \quad (1)$$

Q_{sg} is the syngas flow, Q_{sto_a} is the stoichiometric airflow required to produce complete combustion, and EA is the excess air. The energy content in the air/fuel mixture is given by Equation (2):

$$LHV_{m\_sg} = LHV_{sg} \times \left(\dot{Q}_{sg}/\dot{Q}_m\right) \quad (2)$$

Where LHV_{sg} is the lower heating value of the syngas. The LHV was obtained from the tests carried out in a downdraft gasifier; on average, LHV_{sg} is equal to 5.4 MJ/Nm^3 (22% of CO, 15% H_2, and 2.9% CH_4). The composition has been obtained using the syngas analyzer Gasboard 3100. Other authors report similar values [13,15,22,70,71]. For this composition, the ratio of syngas volume to the air/fuel mixture volume $\left(Q_{sg}/Q_m\right)$ is about 0.45, hence the LHV of air/syngas mixture is 2.43 MJ/Nm^3. Comparable results of air/syngas mixture have been reported by [70] and [72]. From a study carried out by [46], the LHV of the air/gasoline mixture $\left(LHV_{m\_g}\right)$ is 3.6 MJ/Nm^3, the energy content in the air/syngas mixture is two-third of the energy content in the air/gasoline mixture. As the ICE is the same and power derating is attributed mainly to the syngas' lower LHV of mixture air/fuel [5], a power reduction of 30-35% can be expected. This is a gross estimation since the power reduction is also related to other parameters such as the reduction of the laminar flame velocity and the adiabatic flame temperature.

4.3.2. Experimental efficiency evaluation methodology

The system's efficiency can be estimated, employing the relation between total input energy content in the fuel and electrical power production. The electrical power is measured using a Siemens SENTRON PAC3200 power meter. The instantaneous power input in the gasoline operation mode P_{i_g} is estimated as shown the Equation (3).

$$P_{i_g} = \dot{m}_g \times LHV_g \quad (3)$$

And the gasoline mass flow m_g is estimated by Equation (4)

$$\dot{m}_g = (Q_a \times \rho_a)/((A/F)_{st} \times (1 + AE)) \quad (4)$$

Where Q_a is the volume of air going into the engine, measured by a hot wire anemometer. Furthermore, ρ_a is the air density and $(A/F)_{st}$ is the stoichiometric air-fuel ratio [73].

Alternatively, for syngas, $P_{i_{sg}}$ is estimated by Equation (5).

$$P_{i_{sg}} = Q_{sg} \times LHV_{sg} \quad (5)$$

Q_{sg} is the volume of syngas calculated by an anemometer.

5. Results

This section includes simulation and experimental test results. The simulated and the experimental performance of the ICE fuelled on syngas and conventional gasoline are presented, especially regarding engine output power reduction and previous efficiency considerations. The expected performance was determined by specific calculations (as described in section 4.3.1), bibliography review, and simulations through CHEMKIN-PRO.

5.1. Simulation results

5.1.1. Laminar flame velocity and adiabatic flame temperature

In addition to the CR or the rpm, the lower flame velocity of syngas are factors that affect the efficiency of the combustion process [18,20,69]. The results of the laminar flame velocity simulation are shown in Fig. 9. Simulations performed for laminar flame velocity provide values of 29-32 cm/s (ER of 1 to 1.1) for syngas. These values are close to those reported by Oliveira[44], where authors used syngas of similar composition. In the case of gasoline, the

velocity increases to 45 – 50 cm/s. For syngas with a lower LHV, laminar flame speed is reduced to 20 cm/s, as Ouimette et al. [56] reported. This reduction is mainly due to a decrease in the H_2 and CO concentration in the syngas.

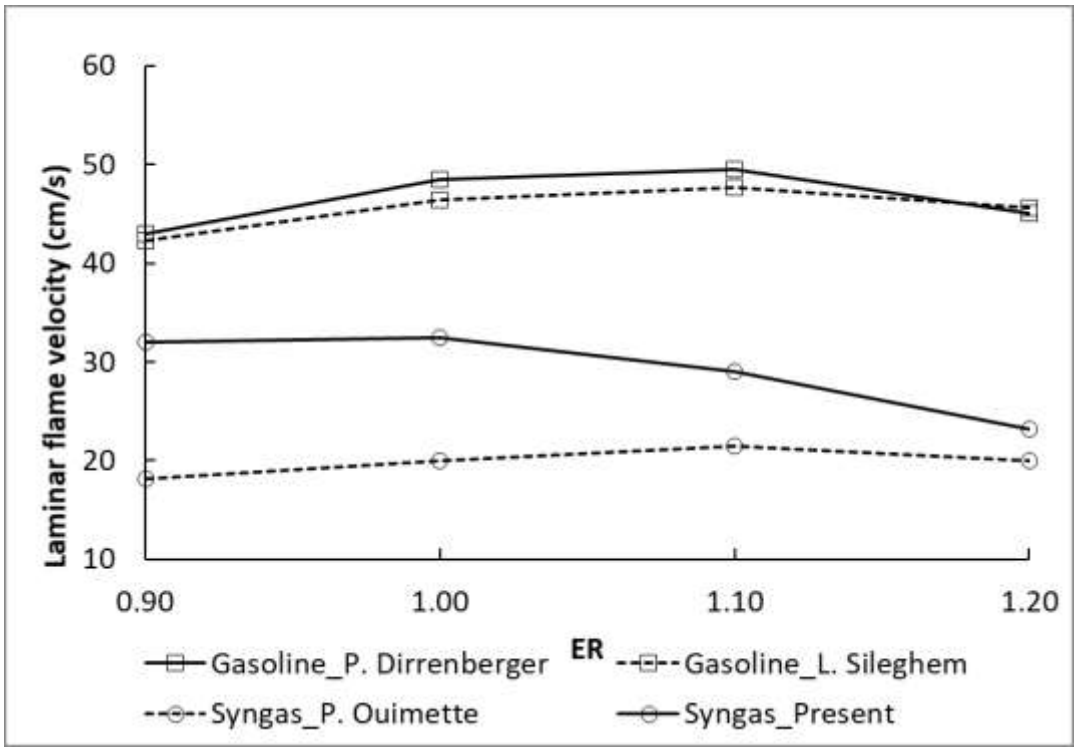

Fig. 9. Comparison of the laminar flame velocity of gasoline and syngas as a function of the ER.

The fuel's adiabatic flame temperature is one factor influencing the engine's efficiency [70]. According to simulations carried out, the analyzed syngas' adiabatic flame temperature is 1885 K (ER 1.05), higher than1750 K reported by Ouimiette et al. [57]. Differences are expected as syngas composition is different (CO and H_2 concentrations are more elevated in the higher adiabatic temperature case). The gasoline adiabatic flame temperature is over 2300 K [74], which is higher than the obtained with syngas. Since a real ICE does not work under ideal conditions, the adiabatic flame temperature cannot be a direct quantitative indicator; hence, an efficiency reduction can be expected for real conditions operation.

5.1.2. Thermal efficiency and power

The simulation results gave information about the efficiency according to rpm, CR, and ignition timing (Fig. 10). Fig. 11 represents the power generation from syngas and gasoline and the impact of the ignition timing on the produced power for syngas (1500 and 3000 rpm, CR 9.3:1 and 11:1) and gasoline (3000 rpm, RC 9.3:1). The tested ICE ignition timing on simulations, expressed in crankshaft degrees, referred to as TDC (top dead center), is -20 (since it occurs before TDC, this value is negative). According to simulations, to obtain the best efficiency for the tested engine (3000 rpm), the best ignition time should be -30° for gasoline and -45° for syngas, reaching thermal efficiency of 18.5% and 16.9%, respectively, in contrast to 14.2% and 17.7% obtained for syngas and gasoline working at -20° referred to TDC (manufacturer adjusted ignition time).

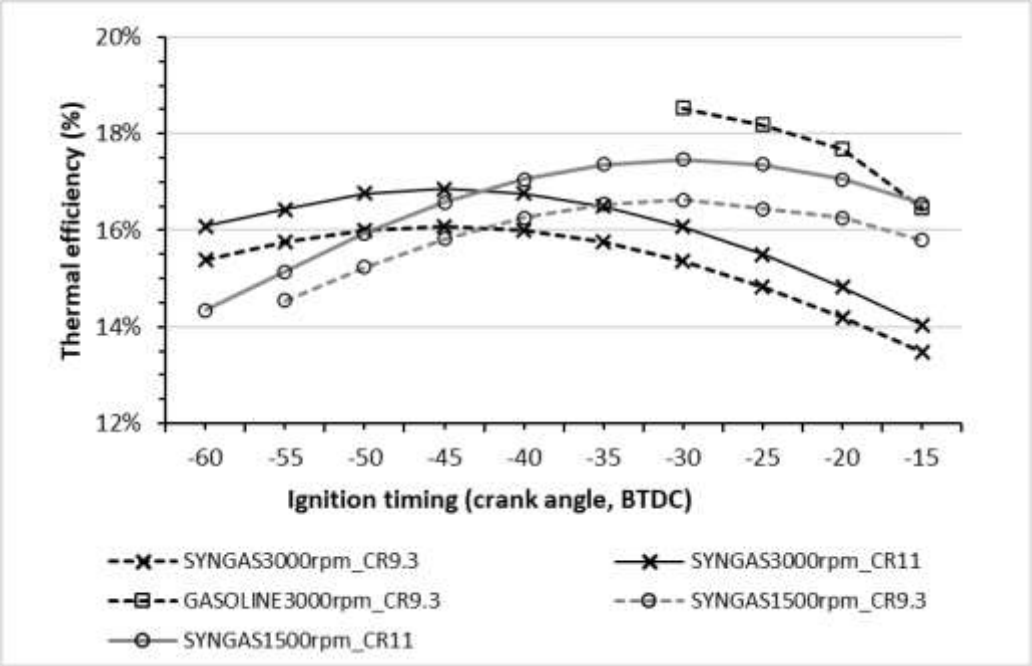

Fig. 10. Thermal efficiency for syngas and gasoline as a function of the ignition timing.

At the real operating conditions of the ICE, the mechanical power reduction working on syngas instead of gasoline is close to 31,4% (from 8.6 to 5.9 kW). If only the CR is increased from 9.3 to 11, the mechanical power could be about 3-4% higher. The same increase would be

obtained working at 1500rpm (Fig. 11). Finally, increasing CR to 11 and reducing the rpm to 1500, the efficiency would increase from 14.2% to 17.5%, but power would be reduced from 6 to 3.4 kW.

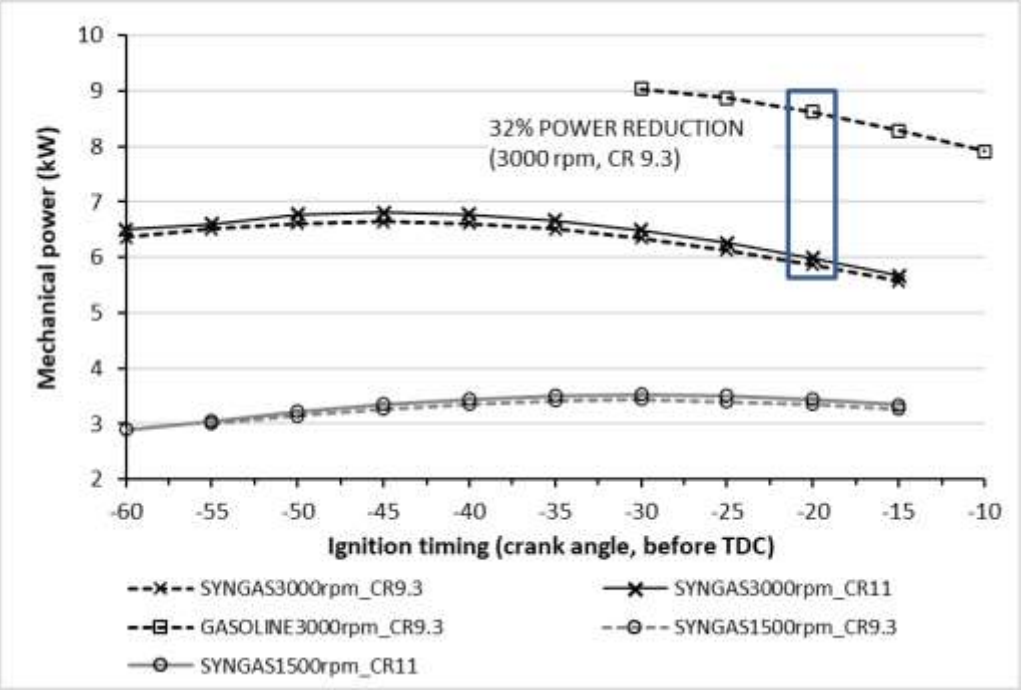

Fig. 11. Mechanical power for syngas and gasoline as a function of the ignition timing.

Simulations were carried out to analyze the engine's behavior according to the ER (Fig. 12 and Fig. 13). Fig. 12 compares the simulations using data inputs of the tested engine. The maximum power for both gasoline and syngas is reached working at the ER from 0.9 to 1. However, to achieve better efficiency and fewer emissions, and working under real conditions, an ICE usually operates at an ER ranged from 1.05 – 1.1 (depending on whether the fuel is liquid or gaseous).

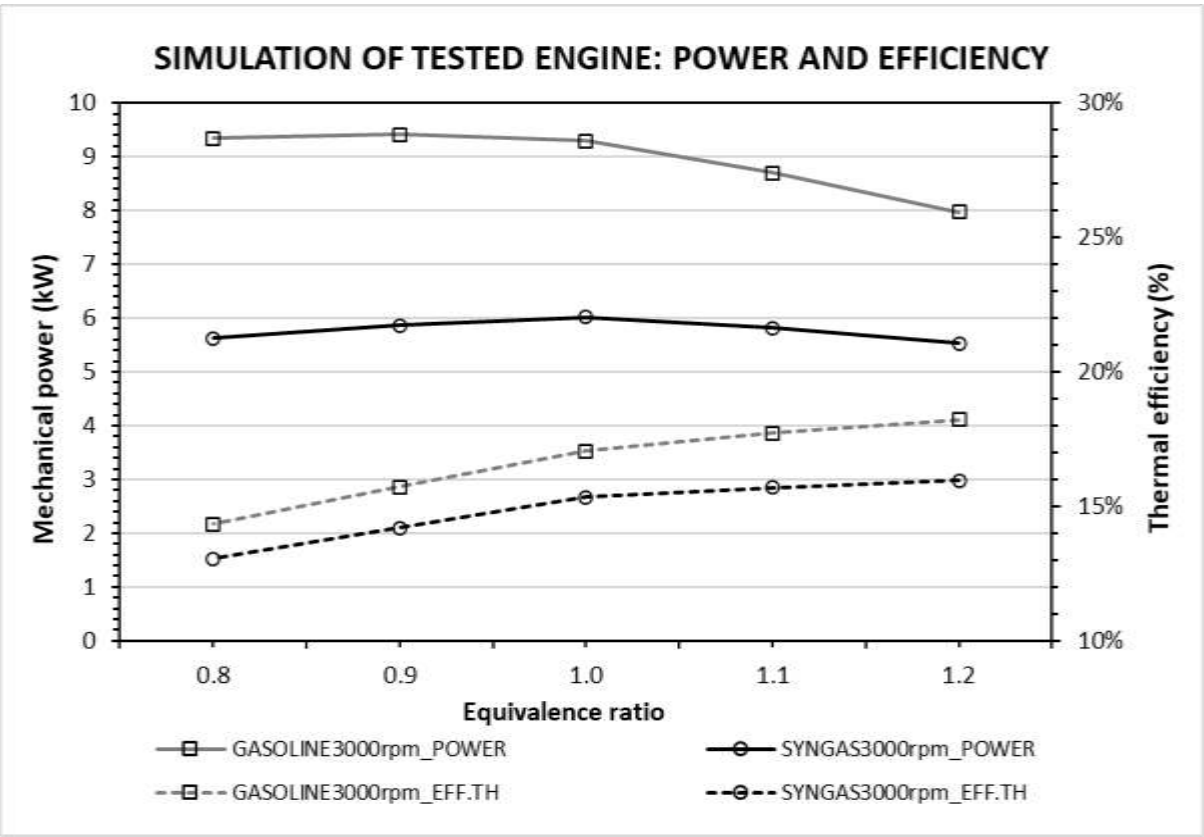

Fig. 12. Power and thermal efficiency performance of the tested engine for gasoline and syngas.

The engine performance optimization, running on syngas at 3000 rpm, would require modifying the ignition time from -20 to -45° referred to TDC (see Fig. 13) and changing the CR from 9.3 to 11. In this case, the engine's thermal efficiency could be increased close to 2.7 percentage points (from 14.2 to 16.9%), and the mechanical power would increase from 5.9 to 6.8 kW (Fig. 13).

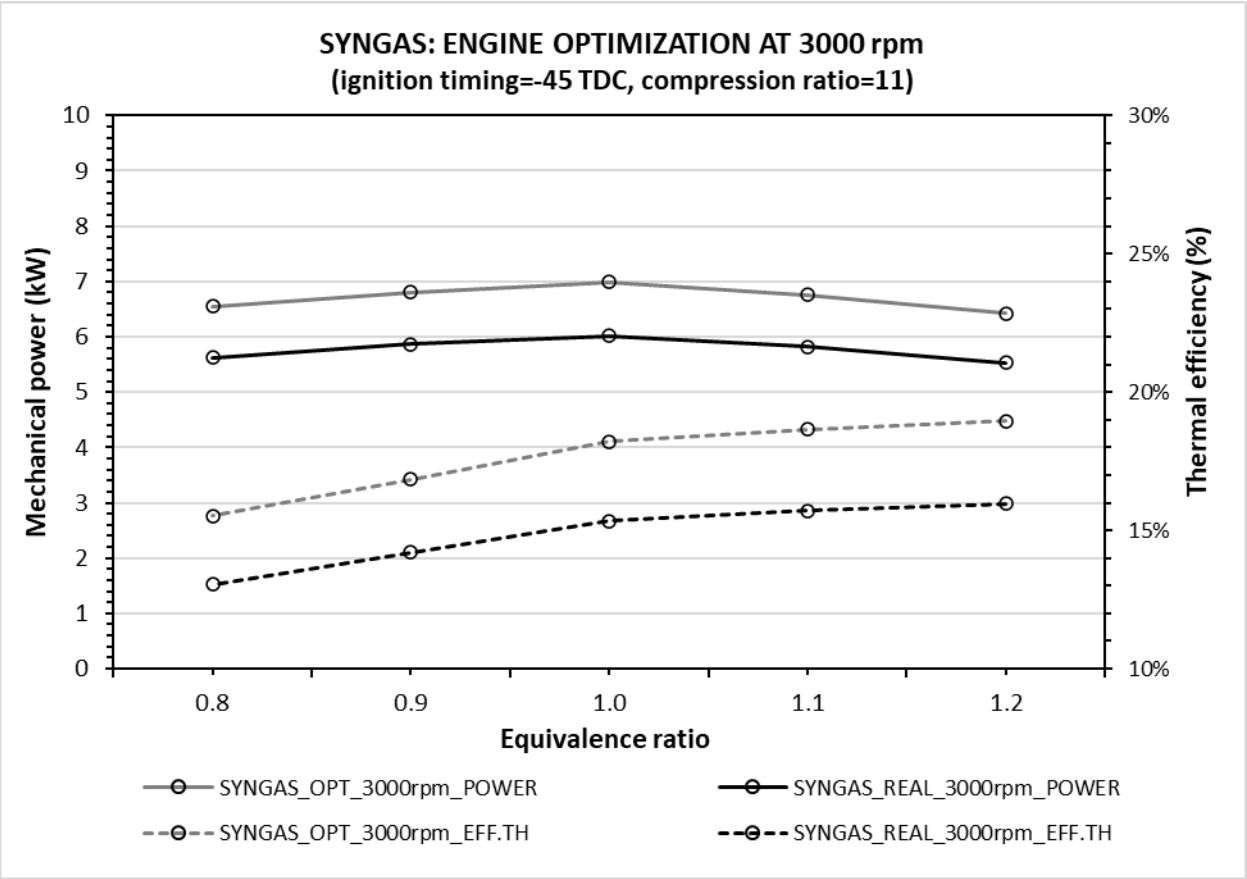

Fig. 13. Engine optimization for syngas (Comparison to engine simulation without modifications).

5.1.3. Torque

The representation of the torque and mechanical power as a function of the ER is shown in Fig. 14. The torque is around 10 and 15.3 N·m per cylinder for syngas and gasoline, respectively, and the maximum torque was obtained for ER ranged from 1 to 1.1. According to manufacturer specifications [47] and real power measured in the experimental tests with gasoline (in point 5.2), maximum torque at 3,000 rpm should be about 16.1 N·m per cylinder, which is in accordance with simulation results of 16.6 N·m per cylinder.

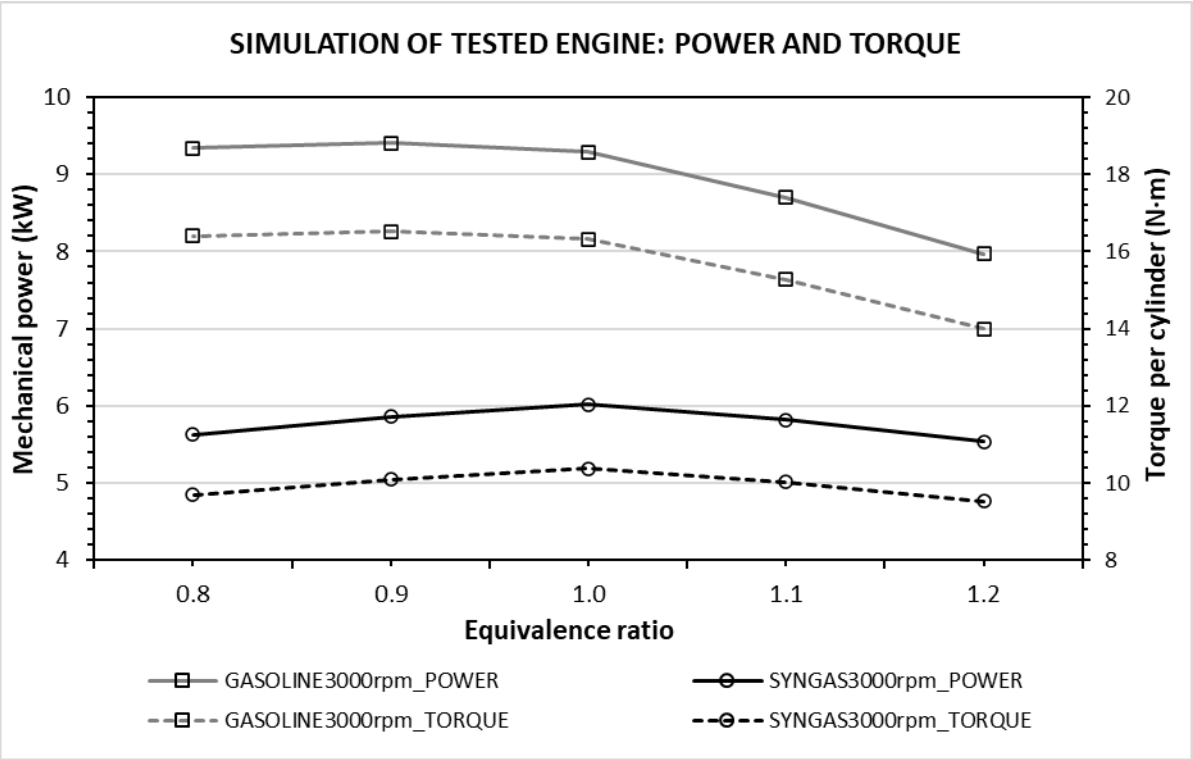

Fig. 14 Power and torque for the tested engine with gasoline and syngas

5.1.4. Emissions

NOx emissions due to gasoline and syngas combustion were obtained from simulations. As syngas flame speed and the adiabatic temperature is lower working on syngas than gasoline, it is also expected lower NOx emission for syngas combustion. In Fig. 15, simulations with the tested engine's data (at 3000 rpm and ignition timing, -20° referred to TDC position) concludes that NO_x emissions are reduced drastically to values lower than 10 ppm. In previous works [19], NO_x measurements for syngas in a small spark-ignition engine (10 kW) were in the range of 20-30 ppm for syngas with an LHV of 6.47 MJ/Nm^3 and methane content of 5.5%V. Considering that tested syngas in this work has lower LHV and methane content is much lower, simulation results are reasonable. On the other hand, considering that the gasoline flame temperature is greater than syngas flame temperature, the NO_x production is smaller when syngas is used as a fuel (see section 5.1.1). NO_x emissions simulation results were also

compared with previous works for small spark-ignition gasoline engines [71], and NO_x emissions were in the range of 700 to 1000 ppm, consistent with simulation results.

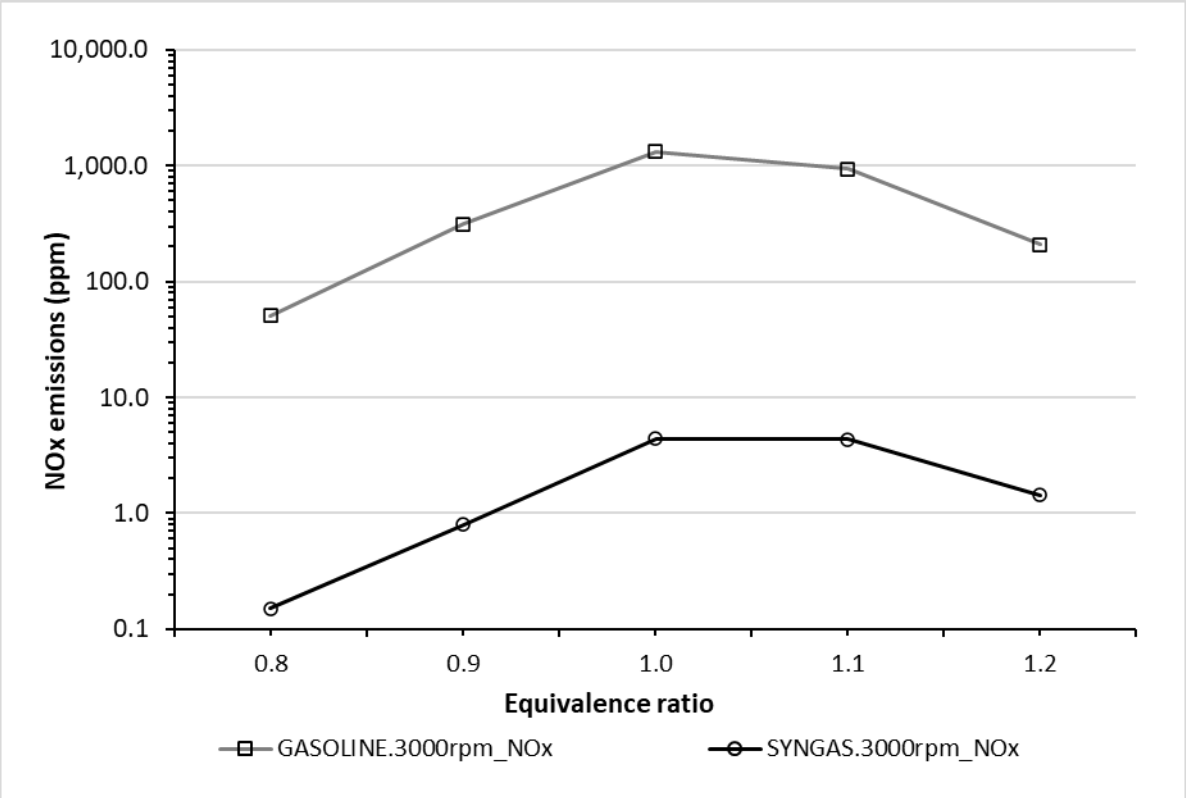

Fig. 15. Comparison of NO_x emissions for the ICE working on gasoline and syngas (logarithmic scale).

5.1.5. Crank angle vs. pressure

The cylinder pressure as a function of the crank angle has also been obtained from the simulations for the ignition time of the ICE under study (-20° referred to TDC position; see Fig. 16). The maximum operating pressures are 3.6 and 4.7 MPa, for gasoline and syngas, reaching such values at 15 and 21° after TDC. These values are in the range of such obtained in previous works [15,65,66]. When running on gasoline, the ICE reaches greater pressure levels than syngas operation, increasing work and power.

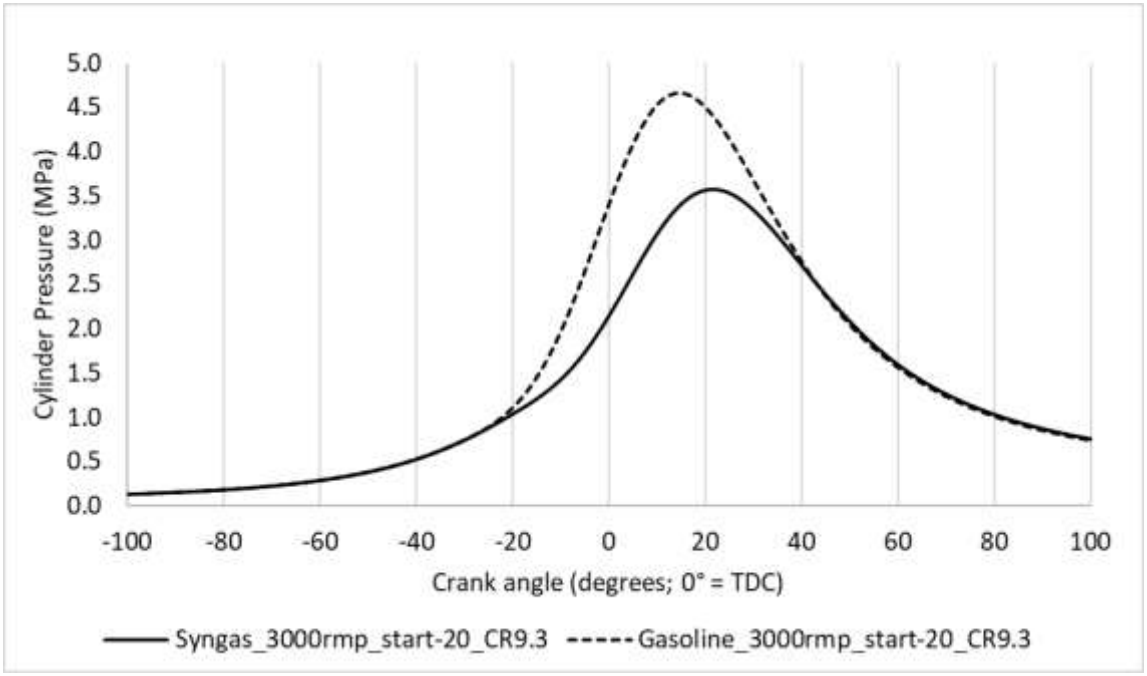

Fig. 16 Evolution of the cylinder pressure as a function of the crank angle

5.2.Experimental results

5.2.1. Efficiency and Electrical power

The conversion efficiency from fuel to electricity of the genset running on gasoline and syngas at different load points are shown in Fig. 17. The overall efficiency of the genset (syngas to electricity) running on gasoline is over 13.7 %, while in the case of the syngas, the efficiency is around 10.5 %. Comparing both fuels at the maximum power reached, the reduction of efficiency was 3.2 percentual points. This reduction can be attributed to the lower adiabatic flame temperature, the slower flame velocity of the syngas, and the non-optimal ignition timing. According to simulations, the ignition timing advance and higher compression ratio would significantly increase efficiency (see 4.1.2). The tested engine CR is 9.3:1; this value is usual for engines running on gasoline, but syngas can work in an engine with a compression ratio of 11:1 [31,75]. According to simulations carried out, increasing CR to 11:1, reducing the rpm to 1500, and improving the ignition timing, the thermal efficiency would increase from 14.2% to

17.5%. Still, mechanical power would reduce from 6 to 3.5 kW. Additionally, according to Equation (2), the air/syngas mixture's energy content is two-thirds of the energy content in the air/gasoline mixture. As the power derating is attributed mainly to the syngas lower LHV of mixture air/fuel [10], a power reduction of 30-35% can be expected.

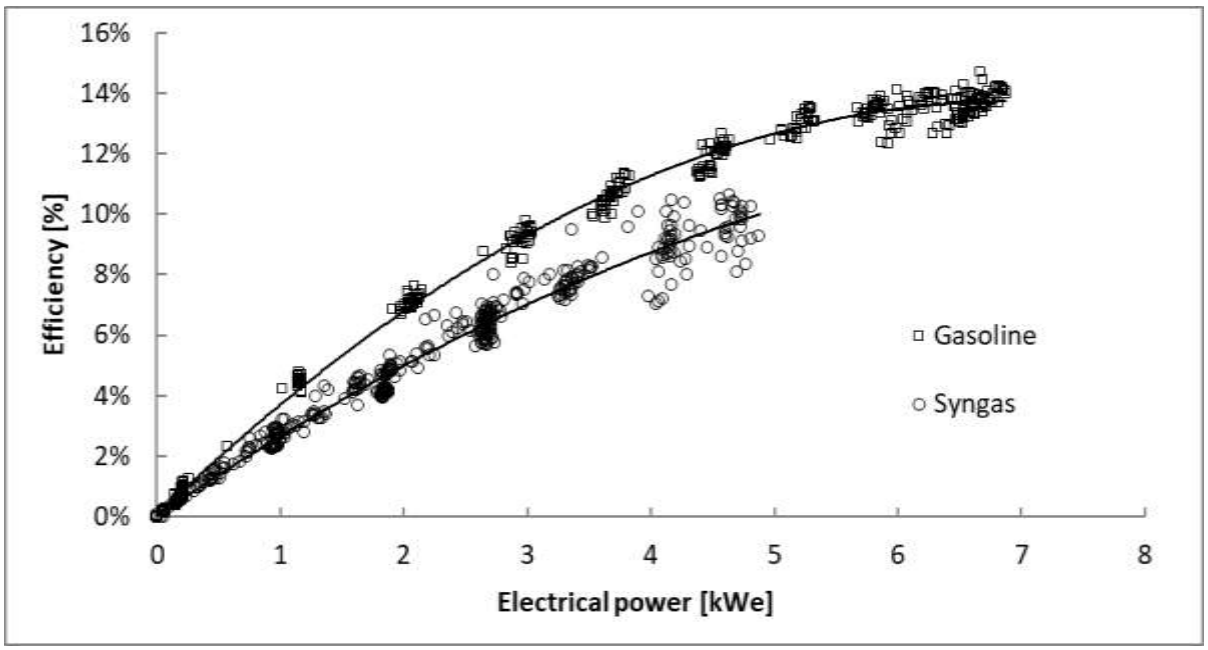

Fig. 17. Overall electrical efficiency of the gasoline engine and syngas engine as a function of the load.

The comparison of the electrical power data for gasoline and syngas is represented in Fig. 18. The maximum electric power reached is higher when the genset runs on gasoline. This value was 6.8 kWe in the test carried out using gasoline, whereas it reached 4.7 kWe when syngas was used. This reduction is mainly produced because of the lower LHV content in the syngas-air mixture compared to the gasoline-air mixture. Besides, in the engine fuelled by syngas, it is observed that for loads bigger than 4.7 kWe, the engine is not able to feed the power demand. It is deduced that the use of syngas reduces the electrical power output by around 30.8% compared to the same genset running on gasoline. This result corresponds with the simulation results previously explained in 5.1.2, where the power reduction reached 31.5%

(From 6.7 to 4.6, taking into account the generator efficiency of 79.5% and the motor-generator coupling efficiency of 97%) with the results obtained for other authors [66,68,76].

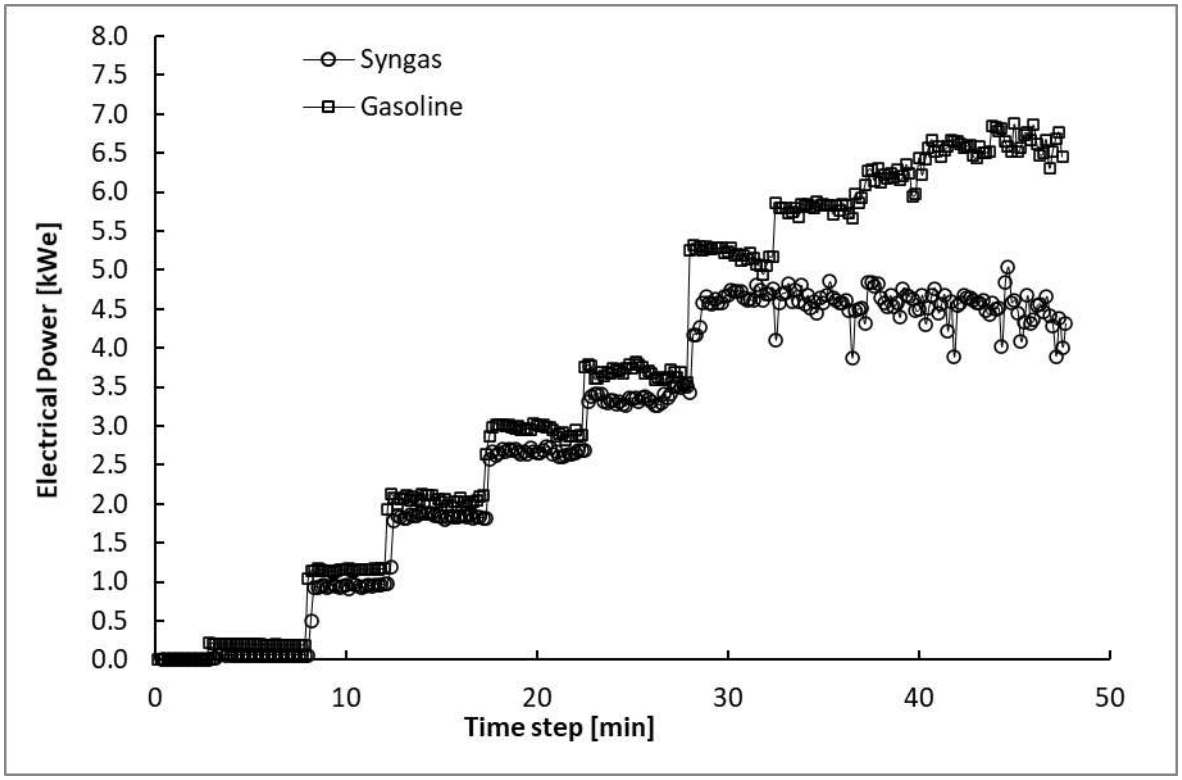

Fig. 18. Electric power evolution for time intervals.

5.2.2. Power quality

The voltage and frequency are represented as a function of the power, as shown in

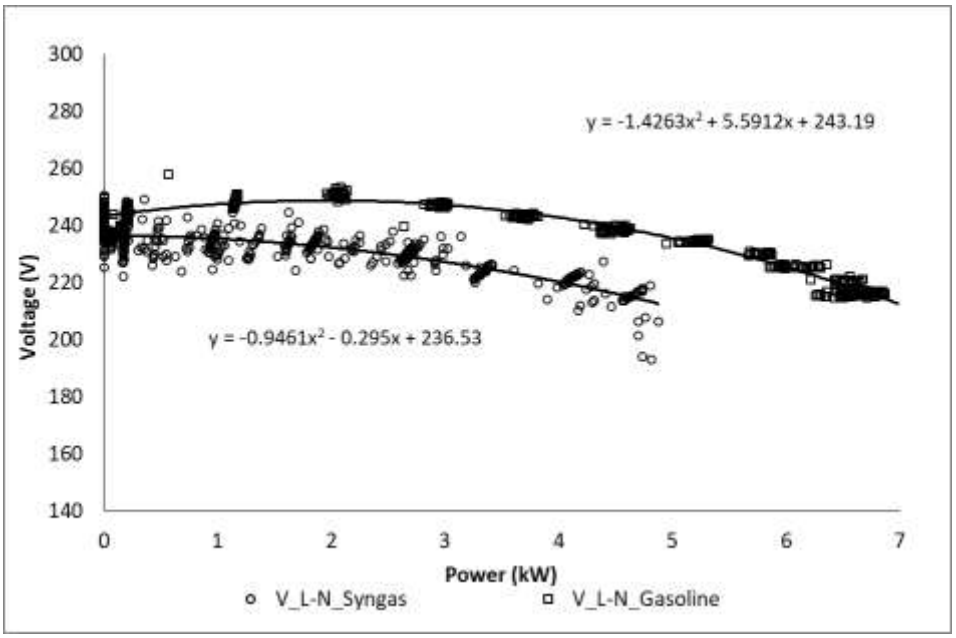

Fig. 19. When the load increases, the voltage of the generator decreases. The generator's nominal voltage is 230 V. Still, at the low load point, the voltage is regulated to 240 - 250 V. Nevertheless, at the maximum electrical power (6.8 kWe for gasoline and 4.7 kWe for syngas), the voltage drops to 215V. The frequency has been represented as a function of the power, as shown in Fig. 20. As with the voltage, when the load power demand increases, the generator's speed decreases and, consequently, its output frequency. The generator's nominal frequency is 50 Hz, but at low load power demand, the frequency reaches its maximum at 52 Hz for gasoline and 51 Hz for Syngas. Nevertheless, the frequency reaches a minimum of 49 Hz for gasoline and 47 Hz for Syngas (at maximum electric power).

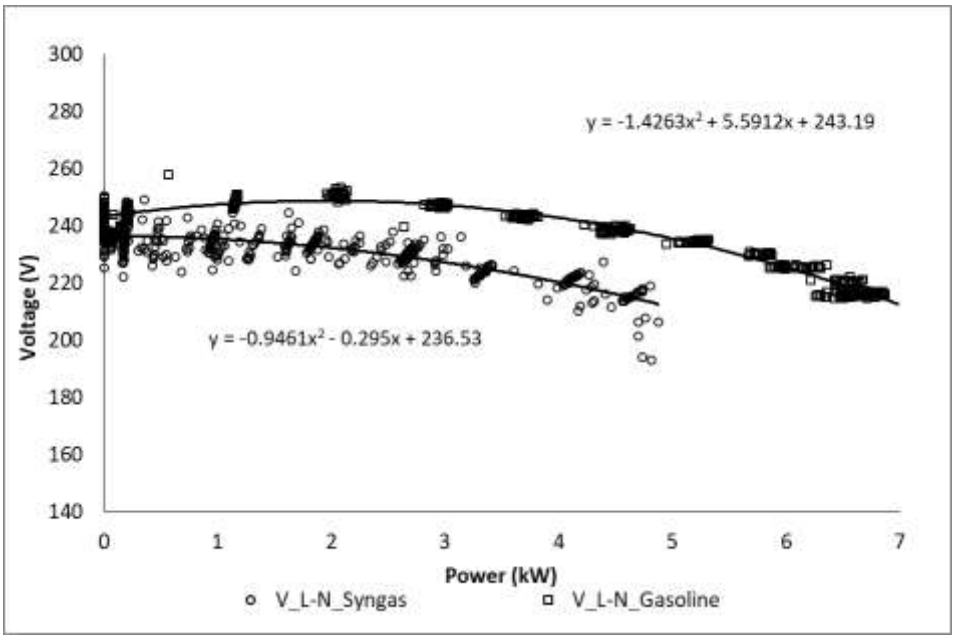

Fig. 19. Behavior of the voltage as a function of the power output.

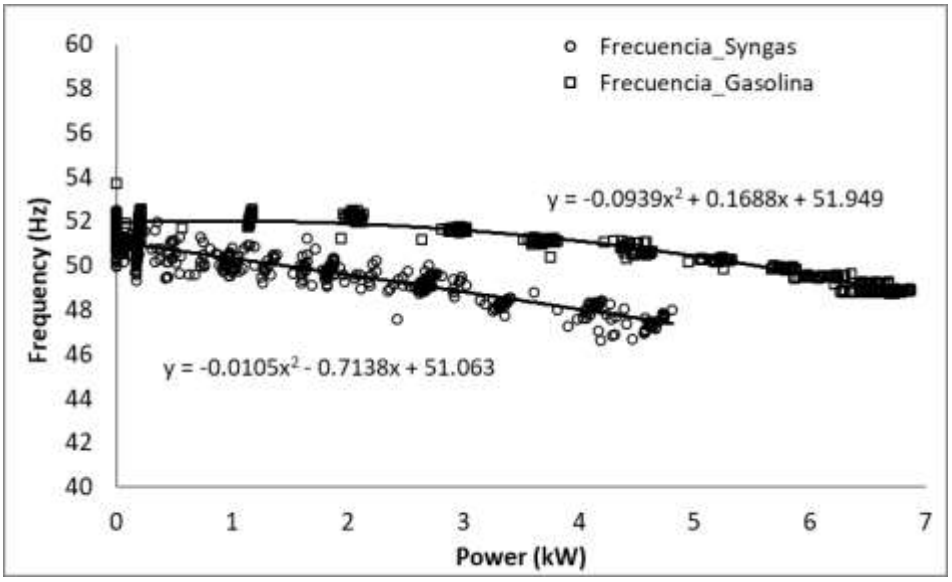

Fig. 20. Behavior of the frequency as a function of the power output.

Since the voltage and frequency behavior is similar when the ICE is running on gasoline or syngas, it can be said that independently of the fuel used, the generator and its regulatory system's characteristics play an essential role in the voltage and frequency quality. Then it depends on the genset voltage and frequency regulation system. Nevertheless, even though the voltage and frequency behavior, the dispersion is more significant when syngas is used. This effect is provoked by the small fluctuations in the LHV and flow of syngas produced by the gasifier.

6. Conclusion and discussion

A comparative study of a genset using gasoline and syngas has been carried out. Through simulation in CHEMKIN- PRO, it was possible to compare for both fuels, laminar flame velocity, adiabatic flame temperature, mechanical power, thermal efficiency, torque, emissions, and pressure as a function of the crank angle and ER. On the other hand, through the experimental test, electrical power and efficiency were analyzed and compared with the

simulations for both fuels. The tests developed show that, technically, converting a gasoline engine to a 100% syngas engine through cheap and straightforward modifications in the inlet manifold but with significant efficiency and power reduction.

According to simulations, at rated operating conditions of the ICE, the mechanical power reduction working on syngas instead of gasoline is close to 31,4% (from 8.6 to 5.9 kW). The thermal efficiency would reduce by 3.5 percentual points (from 17.7 to 14.2%). Considering the alternator efficiency at rated power is 79.5% (data from the manufacturer), and the shaft coupling system's efficiency is close to 98%, the experimental test's conclusions are similar. The experimental test results show that the electrical power output for gasoline operation at rated conditions is 6.8 kW, whereas the syngas mode operation is 4.7 kW (power reduction close to 30.8%). When gasoline is used, 13.7 % of electrical efficiency is reached, whereas if the ICE runs on syngas, the electrical efficiency achieved is 10.5 %. The reduction in electrical efficiency is about 3.2 percentual points. Factors such as lower adiabatic flame temperature, the lower flame velocity of syngas, and non-optimal ignition time strongly influence the efficiency, which is smaller for syngas. It would be possible to increase the efficiency and the power output by modifying the CR and the ignition time angle. Still, it would require significant modification of the genset design that could make the project unfeasible. According to performed simulations for the syngas fuelled engine, increasing the CR to 11, reducing the rpm to 1500, and advancing the ignition time to 30° referred to TDC would increase the thermal efficiency from 14.2% to 17.5%, but the mechanical power would reduce from 6 to 3.4 kW.

Finally, it can be noticed that as the load power demand increases, the voltage and the frequency of the generator decreases. Since this behavior is similar for both fuels, it can be concluded that independently of the fuel used, the generator and its regulatory system's characteristics play an essential role in the voltage and frequency quality. Then it depends on

the genset voltage and frequency regulation system. Nevertheless, even though the voltage and frequency behavior, the dispersion is more significant when syngas is used. This effect is provoked by the small fluctuations in the LHV and flow of syngas produced by the gasifier.

Acknowledgments

The present work was supported in part by the Institute for Energy Engineering of Universitat Politècnica de València.

7. References

[1] J.H. Ng, H.K. Ng, S. Gan, Advances in biodiesel fuel for application in compression ignition engines, Clean Technologies and Environmental Policy. 12 (2010) 459–493. https://doi.org/10.1007/s10098-009-0268-6.

[2] S. Ramalingam, M. Ezhumalai, M. Govindasamy, Syngas: Derived from biodiesel and its influence on CI engine, Energy. (2019). https://doi.org/10.1016/j.energy.2019.116189.

[3] G. Oh, H.W. Ra, S.M. Yoon, T.Y. Mun, M.W. Seo, J.G. Lee, S.J. Yoon, Syngas production through gasification of coal water mixture and power generation on dual-fuel diesel engine, Journal of the Energy Institute. 92 (2019) 265–274. https://doi.org/10.1016/j.joei.2018.01.009.

[4] S. Obara, K. Sato, Y. Utsugi, Study on the operation optimization of an isolated island microgrid with renewable energy layout planning, Energy. 161 (2018) 1211–1225. https://doi.org/10.1016/J.ENERGY.2018.07.109.

[5] L.I. Chaves, M.J. Da Silva, S.N.M. De Souza, D. Secco, H.A. Rosa, C.E.C. Nogueira, E.P. Frigo, Small-scale power generation analysis: Downdraft gasifier coupled to engine generator set, Renewable and Sustainable Energy Reviews. 58 (2016) 491–498. https://doi.org/10.1016/j.rser.2015.12.033.

[6] D. Alfonso-solar, C. Vargas-Salgado, C. Sánchez-díaz, E. Hurtado-pérez, Small-scale hybrid photovoltaic-biomass systems feasibility analysis for higher education buildings, Sustainability (Switzerland). 12 (2020) 1–11. https://doi.org/10.3390/su12219300.

[7] E. Hurtado, E. Peñalvo-López, Á. Pérez-Navarro, C. Vargas, D. Alfonso, A. Pérez-Navarro, C. Vargas, D. Alfonso, Optimization of a hybrid renewable system for high feasibility application in non-connected zones, Applied Energy. 155 (2015) 308–314. https://doi.org/10.1016/j.apenergy.2015.05.097.

[8] C.Y. Acevedo-Arenas, A. Correcher, C. Sánchez-Díaz, E. Ariza, D. Alfonso-Solar, C. Vargas-Salgado, J.F. Petit-Suárez, MPC for optimal dispatch of an AC-linked hybrid PV/wind/biomass/H2 system incorporating demand response, Energy Conversion and Management. 186 (2019) 241–257. https://doi.org/10.1016/j.enconman.2019.02.044.

[9] A. Pérez-Navarro, D. Alfonso, H.E.E. Ariza, J. Cárcel, A. Correcher, G. Escrivá-Escrivá, E. Hurtado, F. Ibáñez, E. Peñalvo, R. Roig, C. Roldán, C. Sánchez, I. Segura, C. Vargas, Experimental verification of hybrid renewable systems as feasible energy sources, Renewable Energy. 86 (2016) 384–391. https://doi.org/10.1016/j.renene.2015.08.030.

[10]C. Chiñas-Palacios, C. Vargas-Salgado, J. Aguila-Leon, E. Hurtado-Pérez, A cascade hybrid PSO feed-forward neural network model of a biomass gasification plant for covering the energy demand in an AC microgrid, Energy Conversion and Management. 232 (2021) 113896. https://doi.org/10.1016/j.enconman.2021.113896.

[11]C.A. Rinaldini, G. Allesina, S. Pedrazzi, E. Mattarelli, P. Tartarini, Modeling and optimization of industrial internal combustion engines running on Diesel/syngas blends, Energy Conversion and Management. 182 (2019) 89–94. https://doi.org/10.1016/j.enconman.2018.12.070.

[12]International Energy Agency, Technology Roadmap: Delivering Sustainable Bioenergy, 2017.

[13]D. Piazzullo, M. Costa, M. Vujanovic, E. Ranzi, M. Costa, Z. Petranovic, L. Villetta, C. Caputo, D. Cirillo, CFD Modelling of a Spark Ignition Internal Combustion Engine Fuelled with Syngas for a mCHP System The 3rd South East Europe Conference on Sustainable Development of Energy, Water and Environment Systems-3rd SEE SDEWES Novi Sad View project Dual fuel comb, in: CHEMICAL ENGINEERING TRANSACTIONS, 2018.

[14]F. Ardolino, U. Arena, Biowaste-to-Biomethane: An LCA study on biogas and syngas roads, Waste Management. 87 (2019) 441–453. https://doi.org/10.1016/j.wasman.2019.02.030.

[15]X. Kan, D. Zhou, W. Yang, X. Zhai, C.H. Wang, An investigation on utilization of biogas and syngas produced from biomass waste in premixed spark ignition engine, Applied Energy. 212 (2018) 210–222. https://doi.org/10.1016/j.apenergy.2017.12.037.

[16]C. Vargas-Salgado, E. Hurtado-Pérez, D. Alfonso-Solar, A. Malmquist, Empirical Design , Construction , and Experimental Test of a Small - Scale Bubbling Fluidized Bed Reactor, Sustainability (Switzerland). 13 (2021) 1–23.

[17]Bahaaddein K M, S.A. Sulaiman, S. Hassan, Syngas Dual-Fuelling, in: Z.A. Abdul Karim, S.A. Bin Sulaiman (Eds.), Alternative Fuels for Compression Ignition Engines, Springer Singapore, Singapore, 2018: pp. 37–52. https://doi.org/10.1007/978-981-10-7754-8_3.

[18]S. Lee, S. Lee, Synthesis Gas, 2017. https://doi.org/10.1201/9780203747469-2.

[19]N. Indrawan, S. Thapa, P.R. Bhoi, R.L. Huhnke, A. Kumar, Engine power generation and emission performance of syngas generated from low-density biomass, Energy Conversion and Management. 148 (2017) 593–603. https://doi.org/10.1016/j.enconman.2017.05.066.

[20]V.S. Yaliwal, N.R. Banapurmath, N.M. Gireesh, P.G. Tewari, Production and utilization of renewable and sustainable gaseous fuel for power generation applications: A review of literature, Renewable and Sustainable Energy Reviews. 34 (2014) 608–627. https://doi.org/10.1016/j.rser.2014.03.043.

[21]J. Arroyo, F. Moreno, M. Muñoz, C. Monné, N. Bernal, Combustion behavior of a spark ignition engine fueled with synthetic gases derived from biogas, Fuel. 117 (2014) 50–58. https://doi.org/10.1016/j.fuel.2013.09.055.

[22]J.D. Martínez, K. Mahkamov, R. V. Andrade, E.E. Silva Lora, Syngas production in downdraft biomass gasifiers and its application using internal combustion engines, Renewable Energy. 38 (2012) 1–9. https://doi.org/10.1016/j.renene.2011.07.035.

[23]A.L. Boehman, O. Le Corre, Combustion of syngas in internal combustion engines, Combustion Science and Technology. 180 (2008) 1193–1206. https://doi.org/10.1080/00102200801963417.

[24]J.R. Copa, C.E. Tuna, J.L. Silveira, R.A.M. Boloy, P. Brito, V. Silva, J. Cardoso, D. Eusébio, Techno-economic assessment of the use of syngas generated from biomass to feed an internal combustion engine, 2020. https://doi.org/10.3390/en13123097.

[25]L. Montuori, C. Vargas-Salgado, M. Alcázar-Ortega, Impact of the throat sizing on the operating parameters in an experimental fixed bed gasifier: Analysis, evaluation and testing, Renewable Energy. 83 (2015) 615–625. https://doi.org/10.1016/j.renene.2015.04.068.

[26]A.M. Shivapuji, S. Dasappa, Influence of fuel hydrogen fraction on syngas fueled SI engine: Fuel thermo-physical property analysis and in-cylinder experimental investigations, International Journal of Hydrogen Energy. 40 (2015) 10308–10328. https://doi.org/10.1016/j.ijhydene.2015.06.062.

[27]J.J. Hernández, M. Lapuerta, J. Barba, Separate effect of H2, CH4 and CO on diesel engine performance and emissions under partial diesel fuel replacement, Fuel. 165 (2016) 173–184. https://doi.org/10.1016/j.fuel.2015.10.054.

[28]J.J. Hernández, M. Lapuerta, J. Barba, Effect of partial replacement of diesel or biodiesel with gas from biomass gasification in a diesel engine, Energy. 89 (2015) 148–157. https://doi.org/10.1016/j.energy.2015.07.050.

[29]R. Chandra, V.K. Vijay, P.M.V. Subbarao, T.K. Khura, Performance evaluation of a constant speed IC engine on CNG, methane enriched biogas and biogas, Applied Energy. 88 (2011) 3969–3977. https://doi.org/10.1016/j.apenergy.2011.04.032.

[30]C.D. Rakopoulos, C.N. Michos, Generation of combustion irreversibilities in a spark ignition engine under biogas-hydrogen mixtures fueling, International Journal of Hydrogen Energy. 34 (2009) 4422–4437. https://doi.org/10.1016/j.ijhydene.2009.02.087.

[31]E. Monteiro, J. Sotton, M. Bellenoue, N.A. Moreira, S. Malheiro, Experimental study of syngas combustion at engine-like conditions in a rapid compression machine, Experimental Thermal and Fluid Science. 35 (2011) 1473–1479. https://doi.org/10.1016/j.expthermflusci.2011.06.006.

[32]Z. Xu, M. Jia, Y. Li, Y. Chang, G. Xu, L. Xu, X. Lu, Computational optimization of fuel supply, syngas composition, and intake conditions for a syngas/diesel RCCI engine, Fuel. 234 (2018) 120–134. https://doi.org/10.1016/j.fuel.2018.07.003.

[33]M.H. Morsy, Modeling study on the production of hydrogen/syngas via partial oxidation using a homogeneous charge compression ignition engine fueled with natural gas, International Journal of Hydrogen Energy. 39 (2014) 1096–1104. https://doi.org/10.1016/j.ijhydene.2013.10.160.

[34]M. Fiore, V. Magi, A. Viggiano, Internal combustion engines powered by syngas: A review, Applied Energy. 276 (2020) 115415. https://doi.org/10.1016/j.apenergy.2020.115415.

[35]L. Wei, X. Li, W. Yang, Y. Dai, C.H. Wang, Optimization of operation strategies of a syngas-fueled engine in a distributed gasifier-generator system driven by horticulture waste, Energy Conversion and Management. 208 (2020) 112580. https://doi.org/10.1016/j.enconman.2020.112580.

[36]V.E. Kozlov, N.S. Titova, I. V. Chechet, Modeling study of hydrogen or syngas addition on combustion and emission characteristics of HCCI engine operating on iso-octane, Fuel. 221 (2018) 61–71. https://doi.org/10.1016/j.fuel.2018.02.062.

[37]Q. Tang, P. Jiang, C. Peng, X. Duan, Z. Zhao, Impact of acetone–butanol–ethanol (ABE) and gasoline blends on the energy balance of a high-speed spark-ignition engine, Applied Thermal Engineering. 184 (2021) 116267. https://doi.org/10.1016/j.applthermaleng.2020.116267.

[38]Y. Zhang, J. Fu, J. Shu, M. Xie, F. Zhou, J. Liu, D. Zeng, A numerical investigation of the effect of natural gas substitution ratio (NGSR) on the in-cylinder chemical reaction and emissions formation process in natural gas (NG)-diesel dual fuel engine, Journal of the Taiwan Institute of Chemical Engineers. 105 (2019) 85–95. https://doi.org/10.1016/j.jtice.2019.09.021.

[39]D. Zhou, W. Yang, J. Li, K.L. Tay, S.K. Chou, M. Kraft, Efficient Combustion Modelling in RCCI Engine with Detailed Chemistry, Energy Procedia. 105 (2017) 1582–1587. https://doi.org/10.1016/j.egypro.2017.03.504.

[40]Y. Rezgui, A sequential CFD-chemistry investigation of the chemical and dilution effects of hydrogen addition on the combustion of PRF-85 in an HCCI engine, Fuel. 292 (2021) 120299. https://doi.org/10.1016/j.fuel.2021.120299.

[41]CHEMKIN, CHEMKIN Tutorials Manual, Reaction Design. (2011) 1–274.

[42]D. Zhou, W. Yang, F. Zhao, J. Li, Dual-fuel RCCI engine combustion modeling with detailed chemistry considering flame propagation in partially premixed combustion, Applied Energy. 203 (2017) 164–176. https://doi.org/10.1016/j.apenergy.2017.06.021.

[43]A. Zehni, R.K. Saray, Comparison of late PCCI combustion, performance and emissions of diesel engine for B20 and B100 fuels by KIVA-CHEMKIN coupling, Renewable Energy. 122 (2018) 118–130. https://doi.org/10.1016/j.renene.2018.01.046.

[44]G.P. Oliveira, M.E. Sbampato, C.A. Martins, L.R. Santos, L.G. Barreta, R.F. Boschi Gonçalves, Experimental laminar burning velocity of syngas from fixed-bed downdraft biomass gasifiers, Renewable Energy. 153 (2020) 1251–1260. https://doi.org/10.1016/j.renene.2020.02.083.

[45]U. Azimov, M. Okuno, K. Tsuboi, N. Kawahara, E. Tomita, Multidimensional CFD simulation of syngas combustion in a micro-pilot-ignited dual-fuel engine using a constructed chemical kinetics mechanism, International Journal of Hydrogen Energy. 36 (2011) 13793–13807. https://doi.org/10.1016/j.ijhydene.2011.07.140.

[46]C.A. Vargas Salgado, Estudio comparativo de la utilización de las tecnologías de gasificación Downdraft y lecho fluidizado burbujeante para la generación de energía eléctrica en aplicaciones de baja potencia, Universitat Politècnica de València, 2012. https://doi.org/10.4995/Thesis/10251/16379.

[47]Honda Engines Europe, Honda GX630 Engines Europe, (2019).

[48]L. Electric, Alternator E1C11M B Single-Phase brushless synchronous with capacitor-2 poles, (2012).

[49]Y. Cao, Q. Wang, J. Du, J. Chen, Oxygen-enriched air gasification of biomass materials for high-quality syngas production, Energy Conversion and Management. 199 (2019) 111628. https://doi.org/10.1016/j.enconman.2019.05.054.

[50]P. Dirrenberger, P.A. Glaude, R. Bounaceur, H. Le Gall, A.P. Da Cruz, A.A. Konnov, F. Battin-Leclerc, Laminar burning velocity of gasolines with addition of ethanol, Fuel. 115 (2014) 162–169. https://doi.org/10.1016/j.fuel.2013.07.015.

[51]L. Sileghem, V.A. Alekseev, J. Vancoillie, K.M. Van Geem, E.J.K. Nilsson, S. Verhelst, A.A. Konnov, Laminar burning velocity of gasoline and the gasoline surrogate components iso-octane, n-heptane and toluene, Fuel. 112 (2013) 355–365. https://doi.org/10.1016/j.fuel.2013.05.049.

[52]Mechanism Downloads - NUI Galway, (n.d.).

[53]Gregory P. Smith, David M. Golden, Michael Frenklach, Nigel W. Moriarty, Boris Eiteneer, Mikhail Goldenberg, C. Thomas Bowman, Ronald K. Hanson, Soonho Song, Jr. William C. Gardiner, Vitali V. Lissianski, Zhiwei Qin, GRI-Mech 3.0, (n.d.).

[54]S.M. Aceves, D.L. Flowers, J. Martinez-Frias, J.R. Smith, C.K. Westbrook, W.J. Pitz, R. Dibble, J.F. Wright, W.C. Akinyemi, R.P. Hessel, A sequential fluid-mechanic chemical-kinetic model of propane HCCI combustion, SAE Technical Papers. (2001). https://doi.org/10.4271/2001-01-1027.

[55]Gregory P. Smith, David M. Golden, Michael Frenklach, Nigel W. Moriarty, Boris Eiteneer, Mikhail Goldenberg, C. Thomas Bowman, Ronald K. Hanson, Soonho Song, Jr. William C. Gardiner, Vitali V. Lissianski, Zhiwei Qin, GRI-Mech 3.0, (n.d.).

[56]M. V. Petrova, F.A. Williams, A small detailed chemical-kinetic mechanism for hydrocarbon combustion, Combustion and Flame. 144 (2006) 526–544. https://doi.org/10.1016/j.combustflame.2005.07.016.

[57]P. Ouimette, P. Seers, Numerical comparison of premixed laminar flame velocity of methane and wood syngas, 2009. https://doi.org/10.1016/j.fuel.2008.10.008.

[58]G.P. Oliveira, M.E. Sbampato, C.A. Martins, L.R. Santos, L.G. Barreta, R.F. Boschi Gonçalves, Experimental laminar burning velocity of syngas from fixed-bed downdraft biomass gasifiers, Renewable Energy. 153 (2020) 1251–1260. https://doi.org/10.1016/j.renene.2020.02.083.

[59]R.J. Varghese, S. Kumar, Machine learning model to predict the laminar burning velocities of H2/CO/CH4/CO2/N2/air mixtures at high pressure and temperature conditions, International Journal of Hydrogen Energy. 45 (2020) 3216–3232. https://doi.org/10.1016/j.ijhydene.2019.11.134.

[60]W. Gardiner, V. Lissianski, Z. Qin, G. Smith, D. Golden, M. Frenklach, B. Eiteneer, M. Goldenberg, N. Moriarty, C. Bowman, R. Hanson, S. Song, C. Schmidt, R. Serauskas, The GRI-Mech(TM) Model for Natural Gas Combustion and NO Formation and Removal Chemistry, Fifth International Conference on Technologies and Combustion for a Clean Environment. (1999) 153–155. http://combustion.berkeley.edu/gri-mech/new21/abstracts/lisbon.pdf.

[61]A. Ergut, S. Granata, J. Jordan, J. Carlson, J.B. Howard, H. Richter, Y.A. Levendis, PAH formation in one-dimensional premixed fuel-rich atmospheric pressure ethylbenzene and ethyl alcohol flames, Combustion and Flame. 144 (2006) 757–772. https://doi.org/10.1016/j.combustflame.2005.07.019.

[62]S.M. Alam, A.T. Wijayanta, K. Nakaso, J. Fukai, K. Norinaga, J. ichiro Hayashi, A reduced mechanism for primary reactions of coal volatiles in a plug flow reactor,

Combustion Theory and Modelling. 14 (2010) 841–853. https://doi.org/10.1080/13647830.2010.517273.

[63]H.J. Curran, Developing detailed chemical kinetic mechanisms for fuel combustion, Proceedings of the Combustion Institute. 37 (2019) 57–81. https://doi.org/10.1016/j.proci.2018.06.054.

[64]J. Gimenez-Lopez, C.T. Rasmussen, H. Hashemi, M.U. Alzueta, Y. Gao, P. Marshall, C.F. Goldsmith, P. Glarborg, Experimental and Kinetic Modeling Study of C2H2 Oxidation at High Pressure, International Journal of Chemical Kinetics. 48 (2016) 724–738. https://doi.org/10.1002/kin.21028.

[65]L. Wei, X. Li, W. Yang, Y. Dai, C.H. Wang, Optimization of operation strategies of a syngas-fueled engine in a distributed gasifier-generator system driven by horticulture waste, Energy Conversion and Management. 208 (2020) 112580. https://doi.org/10.1016/j.enconman.2020.112580.

[66]F.O. Centeno González, K. Mahkamov, E.E. Silva Lora, R. V. Andrade, R.L. Jaen, Prediction by mathematical modeling of the behavior of an internal combustion engine to be fed with gas from biomass, in comparison to the same engine fueled with gasoline or methane, Renewable Energy. 60 (2013) 427–432. https://doi.org/10.1016/j.renene.2013.05.037.

[67]F.A.O. Food, Agricultural Organization. 1986, 1986.

[68]F. V. Tinaut, A. Melgar, A. Horrillo, A.D. De La Rosa, Method for predicting the performance of an internal combustion engine fuelled by producer gas and other low heating value gases, in: Fuel Processing Technology, 2006: pp. 135–142. https://doi.org/10.1016/j.fuproc.2005.08.009.

[69]Food, A.O. of the United Nations. Forestry Dept. Mechanical Wood Products Branch, Wood Gas as Engine Fuel, Food and Agriculture Organization of the United Nations, 1986.

[70]P. Raman, N.K. Ram, Performance analysis of an internal combustion engine operated on producer gas, in comparison with the performance of the natural gas and diesel engines, Energy. 63 (2013) 317–333. https://doi.org/10.1016/j.energy.2013.10.033.

[71]R.K. Wilk, P. Plis, Theoretical and experimental investigation of biomass gasification process in a fixed bed gasifier, in: ECOS 2009 - 22nd International Conference on Efficiency, Cost, Optimization, Simulation and Environmental Impact of Energy Systems, Brazilian Society of Mechanical Sciences and Engineering, 2009: pp. 1807–1816. https://doi.org/10.1016/j.energy.2010.08.039.

[72]S. Dasappa, On the estimation of power from a diesel engine converted for gas operation - a simple analysis, Proceedings of the Seventeenth National Conference on I.C. Engines and Combustion. (2001) 167–174.

[73]J.B. Heywood, Internal Combustion Engine Fundamentals, 1988. https://doi.org/10.1016/s1350-4789(10)70041-6.

[74]M. McAllister, J.-Y. Chen, A.C. Fernandez-Pello, Fundamentals of Combustion Processes, 1st ed., Springer-Verlag New York, 2011. https://doi.org/10.1007/978-1-4419-7943-8.

8. Annex I

Table 11. Previous works analyzing the syngas use in an internal combustion engine

Goal of the paper	ICE fuel	Real test	Simulation	Observations	Ref	year
Analysis syngas production through the gasification of coal water mixture and power generation on dual-fuel diesel engine	Diesel	Yes	No	Coal gasification using water as a gasifying agent	[3]	2019
An investigation on utilization of biogas and syngas produced from biomass waste in premixed spark ignition engine	-	yes	no	A 25 kW ICE was used CR=12.9, Crank angle as a function of the ER, and adiabatic temperature of flame are not analyzed.	[15]	2018
Combustion behavior evaluation of a spark-ignition engine fueled with synthetic gases derived from biogas	Gasoline	yes	yes	Syngas obtained from catalytic decomposition of biogas.	[21]	2014
Analysis of syngas production in downdraft biomass gasifiers and its application using internal combustion engines	Diesel	Yes	No	Focused on syngas production. General information of the ICE behavior.	[22]	2012
Techno-economic assessment of the use of syngas generated from biomass downdraft gasifier for electricity generation in a 15 kWe internal combustion engine	-	No	No	Focused on Techno-economic assessment.	[24]	2020
Impact of the throat sizing on the operating parameters in an experimental fixed bed gasifier coupled with an internal combustion engine: Analysis, evaluation and testing	-	Yes	No	Focused on the optimization of the gasification process	[25]	2015
Analysis of the influence of fuel hydrogen fraction on syngas fueled SI engine: Fuel thermo-physical property analysis, energy balance and in-cylinder experimental investigations	Diesel	Yes	Yes	7.8 kW, 2- cylinders ICE. Focus on Hydrogen influence in the combustion process. CR= 18.5:1	[26]	2015
Evaluation of the separate effect of H2, CH4, and CO addition on the performance, combustion efficiency, and pollutant emissions of a diesel engine	Diesel	Yes	No	Use a mixed fuel	[27]	2016
Impact evaluation of partial replacement of diesel or biodiesel with gas from biomass gasification in a diesel engine	Diesel	Yes	No	Use a mixed fuel	[28]	2015
Performance evaluation of a 5.9 kW stationary diesel engine converted into spark ignition mode and run on compressed natural gas (CNG), methane enriched biogas (Bio- CNG), and biogas produced from bio	Diesel	Yes		The fuel is CNG enriched whit syngas	[29]	2011

methanation of jatropha and Pongamia oil seed cakes						
Demonstration of the spatial distribution inside the burned gas of the combustion-generated irreversibilities under biogas-hydrogen mixtures fueling.	-	No	Yes	biogas–hydrogen mixtures fueling	[30]	2009
Experimental study of two typical mixtures of H2, CO, CH4, CO2, and N2 coming from a producer gas ananalysis of its turbulent combustion in engine-like rapid compression machine.	-	Yes	Yes	Rapid compression ICE	[31]	2011
Computational optimization of the operating parameters, including fuel supply, syngas composition, and intake conditions of a syngas/diesel RCCI engine under wide load by integrating the KIVA-3V code.	Diesel	No	Yes	Focus on optimizing the parameters of the engine	[32]	2018
Modeling study on the production of hydrogen/syngas via partial oxidation using a homogeneous charge compression ignition engine fueled with natural gas. Analysis of different engine operation parameters impact.	Natural gas	No	Yes	Analyzes the hydrogen/syngas yields	[33]	2014